Geophys. J. R. astr. Soc. (1979) **56**, 159–197

The tidal dynamics of the Irish and Celtic Seas

I. S. Robinson* *Institute of Oceanographic Sciences, Bidston Observatory, Birkenhead, Merseyside*

Received 1978 July 11; in original form 1978 May 25

Summary. Current meter data collected over periods of more than 14 day from the Irish and Celtic Seas are harmonically analysed and presented in maps of tidal stream information. Making use of the analysed current data, and by constructing time series of frictional and inertial stresses which are also harmonically analysed, harmonic constituents of the surface tidal slopes at current meter stations are obtained. Using these with data collected from offshore tide gauges, and in conjunction with coastal tide data, cotidal maps are drawn with some confidence for M_2, S_2, O_1 and K_1, the M_2 chart resolving the discrepancy which exists between the different charts of the Celtic Sea already produced. Cotidal maps for M_3 and M_4 are also presented.

The mean over a tidal cycle of the energy flux for M_2, S_2 and O_1 is also presented in the form of the total energy flux in these constituents which crosses different sectional lines. A flux of 44×10^6 kW is observed to enter the Celtic Sea from the Atlantic and this is compared with previous estimates. An energy budget is also performed for M_2, including all the effects of astronomical forcing and Earth tides to enable comparison to be made between the true energy inflow and the estimated frictional dissipation. Finally, comparison is made between the mean of the instantaneous energy flux and the sum of the energy fluxes associated with the major harmonics.

1 Introduction

Tidally driven water movements dominate the physical oceanography of the Irish Sea, with typical tidal streams of magnitude 1 m/s and ranges of tidal elevation up to 9 m. Temperature and salinity distributions are controlled very much by tidal mixing. Residual flows in the Irish Sea, whether due to horizontal density gradients, tidal non-linearity, differences in mean water level between the North and South Exits, a mean wind stress or any other cause, cannot be realistically modelled in isolation but must be treated as part of the total tidally oscillating system. Since the residuals are typically an order of magnitude, or even two orders of magnitude less than the maximum tidal streams, this places strict

* Present address: Department of Oceanography, University of Southampton, Southampton SO9 5NH.

requirements of accuracy on any analytic or numerical models, and particularly on the boundary conditions used, if residual flows are to be represented at all accurately. The same problem is encountered in the observation of currents, instrumental and rig-induced noise resulting from the tidal streams is the same order as the true residual flows. Even in the case of storm surges where wind-driven currents approach the magnitude of tidal streams and their basic dynamics can be considered in isolation, any second-order analysis must include the surge-tide interaction. What is true of currents is also true of elevations; the observation of mean sea-level requires careful tidal analysis of elevation records, whilst coastal geodesy and hydrodynamic levelling must take into account non-linear tidal set-up and the residual currents mentioned above. Clearly, then, an accurate knowledge of the tidal regime in the Irish Sea, as in any continental shelf area having large tides, is of central importance to all other aspects of its physical oceanography.

Much has been known about the tides of the Irish Sea for the last 50 years, from coastal tide gauges, and from tidal stream observations by the Hydrographic Office of the British Admiralty which are included on navigation charts. Doodson & Corkan (1932), using these observations, constructed a cotidal chart of the Irish Sea for M_2 which has proved to be remarkably accurate, despite the rather crude nature of the tidal stream data available to them. Doodson, Rossiter & Corkan (1954) were able to derive a similar chart from coastal elevation data alone, using a hand-calculated finite difference numerical model of the sea. However, the most recent Admiralty cotidal chart (No. 5058), based on the Spring range, shows differences from this earlier work, producing some uncertainty as to which is the more accurate. As early as 1918, G. I. Taylor (1919) produced his calculations of the tidal energy flux into the Irish Sea and a consequent estimate of a coefficient of quadratic bottom friction, which have contributed much to the study of both global tidal dissipation and the bottom drag on tidal currents. The actual numerical values he obtained must nonetheless be treated with caution in view of the crude tidal stream data available to him. Bowden (1955) summarized the existing knowledge of tides and tidal streams in the Irish Sea. Defant (1961) gave a general description of the tidal dynamics of the area. Since then very little new tidal information has been published, apart from the occasional reporting of new tidal harmonic constants for an Irish Sea port following an Admiralty tide survey.

Nonetheless, there is still much interest in the oceanography of the Irish Sea, and some of the aspects being actively investigated are dependent on an accurate knowledge of the tides. The horizontal temperature and salinity distributions and the existence of the seasonal thermocline depend on the tidal mixing (Simpson, Hughes & Morris 1977) and any modelling of thermocline development requires good tidal stream data. A three-dimensional finite difference model of the Irish Sea has been developed by Heaps (see, e.g. Heaps & Jones 1975) which can ultimately be used to study a variety of dynamical processes, but which depends on accurate tidal information at its boundaries, and at points in its interior for tuning purposes. Accurate cotidal maps for other constituents as well as M_2 are required if observations of Earth tides, particularly the load tide due to the weight of the Irish Sea displacing the Earth's crust, are to be interpreted to yield information about the geophysical structure of Wales and the North of England (see, e.g. Baker & Lennon 1977).

Since 1969, several research cruises in the Irish Sea have been organized by the Bidston Laboratory of the Institute of Oceanographic Sciences. One of these was the British Irish Sea Oceanographic Project (BISOP) which ran in collaboration with several other research institutes. During these cruises current meter moorings were laid, having up to three self-contained recording current meters at different depths in the water column, supported by a sub-surface buoy. These were left for periods of at least 14 day, and mostly over 30 day before recovery, enabling a lunation of tidal current data to be recorded. The cruises also

provided opportunity for deployment of the offshore tide gauge capsules being developed during this period, which recorded sea-bed pressure for a period of up to 30 or more days before recovery. The primary purpose of each cruise and its associated current meter and tide gauge moorings included the intercomparison of different types of current meter, the observation of residual flows through the Irish Sea, the observation of storm surge propagation to provide input data for numerical models and the observation of frontal zones. In 1973 a line of current meters and an offshore tide gauge were placed between St Ives and Cork with the express purpose of studying the tidal regime of the Celtic Sea and, more recently, individual moorings have been placed during cruises to fill gaps in the overall information coverage of the Irish Sea. Other gaps in the nothern Irish Sea have been filled with data supplied by the Fisheries Laboratory at Lowestoft from records of their Irish Sea cruises (Baxter & Bedwell 1972). Results already published from these current observations include Howarth (1975), Flather & Heaps (1975) and Ramster & Howarth (1975). Details of the data and references to sources will be given in the next section.

Because of the availability of such a wide coverage of current meter data capable of analysis into at least the major tidal constituents, and of some offshore elevation data, coupled with the need for reliable tidal information in an accessible form, it was considered worthwhile to process the data and repeat the earlier work of Doodson & Corkan to produce a cotidal map of the Irish Sea for the M_2 constituent, based on much more reliable observations than were available 40 years ago. Moreover, because of the length of data records available, cotidal maps of other constituents could also be produced, and with the benefits of high-speed computing, non-linear effects could be considered and thus an attempt made at producing cotidal charts for shallow-water harmonics. Similarly the work of G. I. Taylor, in evaluating energy fluxes and frictional dissipation, could be confirmed and extended using the modern data, thus enabling the tidal dynamics of the Irish Sea to be explored in more detail. The results of this work are described in the rest of this paper.

2 The data

Fig. 1 shows the coverage of moorings throughout the Irish Sea from which current data were used in the present survey. Although there have been considerably more current meter moorings than are shown in Fig. 1, those with less than 13 days' data have been eliminated. For most of the moorings useful data are available from current meters at more than one depth. Table 1 lists the moorings with their geographical position, the depth of meters, the period over which the data were gathered and reference where available to a more comprehensive description of the operation of the meters, from which possible errors can be deduced. If a serious malfunction of a meter was apparent (e.g. a scatter plot revealing a compass error or spikiness of the time series plot at maximum current revealing interference with the meter by the mooring rig) it was eliminated from the survey, but such detailed analysis is not available for all of the records which have been used. The current meters recorded instantaneous direction and the integrated rotor count since the previous record, usually at 10 min intervals. For this survey, however, the data were obtained in the already reduced form of hourly values of east and north components. For the 1969 'Lowestoft' data, hourly averages of the 10 min east and north resolved current values were used, and timing corrections applied to obtain values on the hour, using a simple quadratic fit between the three nearest nominal hourly values. For the rest of the data, hourly values were obtained, with timing correction, by a 6-point Lagrangian interpolation formula operating on 10 min values filtered to remove high frequency (instrumental and digital) noise. It is considered that the tidal signal should not be significantly affected by either process.

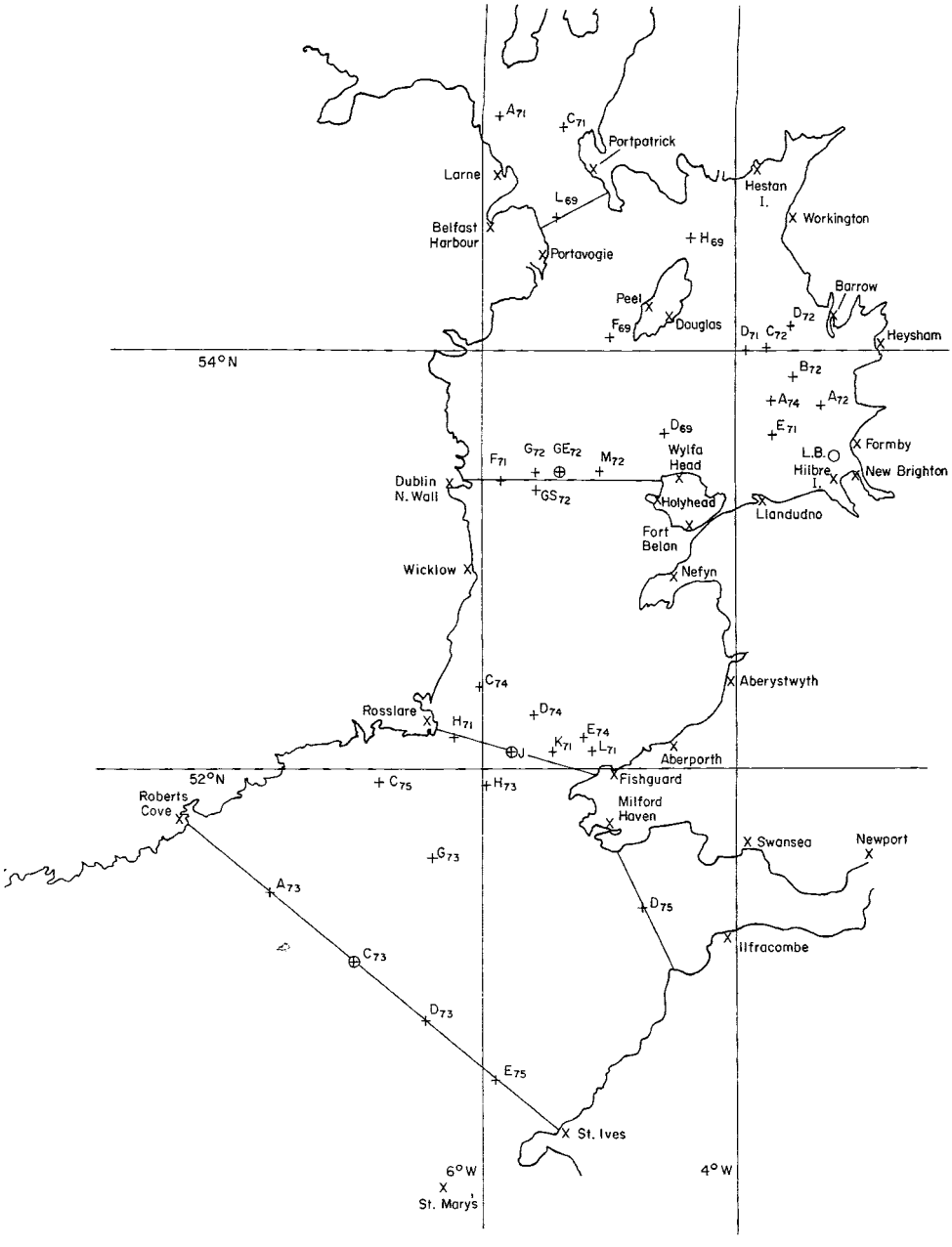

gure 1. Map of data stations and energy flux boundary lines. X Coastal tide gauge. O Offshore tide ıge. + Current meter rig.

Offshore elevations were measured at the four moorings of an offshore tide gauge licated in Fig. 1. The details of each mooring are shown in Table 2. For this survey the ta were obtained in their processed form of tidal harmonic constituents, using the luction and analysis of Alcock & Vassie (1975).

Coastal elevation data were also obtained in the form of tidal harmonic constituents all the ports and tide gauge stations indicated on Fig. 1. Most of these are held in the

Table 1. Current meter mooring details.

Name of Station	Position		Depth of sea bed below chart datum	Height of meters above sea bed (m) (* did not produce a record of the length indicated in column 6)			Period of data collection	Record length used in harmonic analysis	Literature reference	Reference port for related constituents
	Lat.	Long.	(m)	Top	Middle	Bottom		(days)		
C71	55°02'N	5°19'W	73	60*,	33,	5	31/08-10/10/71	30	(2, 3)	Portpatrick
A71	55°05'N	5°50'W	91	79,	42,	5	31/08-10/10/71	30	(2, 3)	Portpatrick
L69	54°38'N	5°23'W	82		66,	5	12/11- 9/12/69	27	(1)	Portpatrick
H69	54°32'N	4°20'W	42		24,	5	12/11-10/12/69	28	(1)	Portpatrick
F69	54°04'N	4°59'W	66	66,	5,	5	12/11-10/12/69	28	(1)	Holyhead
D69	53°39'N	4°34'W	73	69.	38		12/11-10/12/69	28	(1)	Holyhead
D71	54°00'N	3°54'W	35	15,	5,	5	07/09-19/09/71	13	(2)	Douglas
D72	54°07'N	3°33'W	22		13,	5	12/10-30/10/72	15	(5)	Douglas
C72	54°01'N	3°44'W	33	25,	15,	5	12/10-30/10/72	15	(5)	Douglas
B72	53°53'N	3°32'W	22		13,	5	12/10-31/10/72	15	(5)	Hilbre
A72	53°45'N	3°19'W	15		7,		12/10-30/10/72	15	(5)	Hilbre
A74	53°46'N	3°43'W	35	20,		10	16/2-20/3/74	33	(7)	Hilbre
E71	53°36'N	3°42'W	35		23,	5	07/09-20/09/71	14	(2)	Hilbre
M72	53°26'N	5°03'W	95	79,	53		07/09-08/10/71	32	(4)	Holyhead
GE72	53°26'N	5°22'W	83	72,		7	07/09-09/10/72	33	(4)	Holyhead
G72	53°26'N	5°33'W	78	68,		7	07/09-08/10/72	32	(4)	Holyhead
F71	53°24'N	5°50'W	42		30,	5	07/09-19/09/71	13	(2)	Holyhead
GS72	53°21'N	5°33'W	76	66,	40		07/09-09/10/72	33	(4)	Holyhead
C74	52°24'N	6°00'W	55		35,	20*	18/02-19/03/74	30	(7)	Fishguard
D74	52°16'N	5°35'W	93	73,		20	18/02-19/03/74	30	(7)	Fishguard
E74	52°09'N	5°11'W	57			20	09/02-19/03/74	30	(7)	Fishguard
L71	52°05'N	5°08'W	48		20		06/09-21/09/71	16	(2)	Fishguard
K71	52°05'N	5°26'W	73		33,	5*	30/08-03/10/71	30	(2, 3)	Fishguard
H71	52°10'N	6°12'W	68		29,	5	30/08-23/09/71	25	(2, 3)	Fishguard
J74	52°05'N	5°46'W	91	71,	20		19/02-19/03/74	29	(7)	Fishguard
H73	51°55'N	5°58'W	100	80,	65,	15	04/06-06/07/73	33	(6)	St. Mary's
D75	51°19'N	4°44'W	55		35*,	15	22/08-04/10/75	30	(7)	Fishguard
C75	51°56½'N	6°47'W	62		40,	35	17/08-17/09/75	29	(7)	Fishguard
G73	51°34'N	6°23'W	90	70,	55,	15	04/06-17/06/73	14	(6)	St. Mary's
A73	51°24'N	7°40'W	82	64,		15	04/06-05/07/73	32	(6)	St. Mary's
C73	51°03'N	7°00'W	95	73,	58,	15	03/06-05/07/73	33	(6)	St. Mary's
D73	50°45'N	6°27'W	97	75,	60,	15	03/06-05/07/73	33	(6)	St. Mary's
E75	50°27'N	5°54'W	73		55		19/08-06/10/75	30	(7)	St. Mary's

References:

(1) Baxter & Bedwell (1972).
(2) BISOP Data Report, M. J. Howarth (ed.).
(3) Howarth & Loch (1973).
(4) Howarth & Loch (1974a).
(5) Howarth & Loch (1974b).
(6) Howarth & Loch (1974c).
(7) M. J. Howarth, private communication.

records of tidal analyses performed by the Institute of Oceanographic Sciences laboratory at Bidston Observatory. Some of these are the result of a special siting of a temporary tide gauge for a period of three to six months, using a Neyrpic bubbler pressure gauge (Pugh 1971). Mostly they are the constituents used for routine commercial tide predictions at ports having a stilling well and float recording gauge. At none of these ports was less than one month's data used for the analysis and for many ports a year's data have been used. The coverage provided by the Bidston records was supplemented by any additional analyses available from the published records of the International Hydrographic Bureau (1974).

Table 2. Offshore tide gauge moorings.

Name of Station	Position Lat.	Position Long.	Depth of sea bed below chart datum m.	Period of mooring	Length of useful data (days)	Reference port for related constituents
L.B.	53°30'N	3°13'W	9.9	4.6.73 – 23.7.73	36½	Hilbre I.
GE_{72}	53°26.5'N	5°22'W	85	7.9.72 – 10.10.72	31	Holyhead
J_{74}	52°06'N	5°48'W	94	17.2.74 – 20.3.74	24½	Fishguard
C_{73}	51°02.9'N	6°56.6'W	95	2.6.73 – 6.7.73	32	St. Mary's

HARMONIC ANALYSIS

Tidal harmonic analysis of the east and north components of current was performed by the standard least squares algorithm used at Bidston for the routine analysis of coastal elevation time series. This assumes an elevation of the form

$$\zeta = Z_0 + \sum_{n=1}^{N} f_n H_n \cos | V_n + u_n - g_n | + \text{random noise.}$$

Z_0 is mean sea-level, H_n is the amplitude of the constituent whose argument is $V_n = V_{0_n} + \sigma_n t$. σ_n is the frequency and V_{0_n} is chosen so that the phase lag g_n is relative to the phase of the same harmonic constituent of the equilibrium tide (e.g. the time origin for M_2 would be the upper or lower transit of the moon at the Greenwich meridian. Any place with the M_2 signal at a maximum at this time would have $g = 0$). f_n and u_n are corrections to the amplitude and phase of each constituent to take account of the 18.61-yr cycle of the regression of the lunar nodes which cannot be obtained from spans of data having a length of only a few months or a year. They are calculated according to the equilibrium tide relationships. Where a year's data are available, the 60 most important astronomical and shallow water frequencies are normally incorporated into the least squares fit. Where a shorter span of data are to be analysed, the method cannot resolve all of these, and if a non-resolved component is considered to be important to the analysis, it may be obtained by assuming that its relationship in amplitude and phase to another suitable constituent which can be resolved is the same as at a nearby port for which a year's data span, and hence a full analysis, are available.

The harmonic analysis algorithm was applied to the east and north currents as separate time series. Table 3 indicates the constituents required from different spans of data. In all cases some related constituents were necessary to produce the best analysis possible with the length of data available. However, the application of relations based on an elevation analysis to currents must be treated with caution because tidal streams do not necessarily respond in the same way as elevations to the tide generating forces, and therefore it cannot be assumed that there is a simple relationship between currents and elevation at a particular place. Only if the tide could be considered as a linear system composed of simple progressive waves of different frequencies superposed upon each other would it be correct to relate elevations and streams, since they would then be functionally related. In such a case, it would be necessary to assume that the waves were all travelling in the same direction, so that the ratio between east- and north-flowing components of current would be the same for each harmonic constituent. Rearranging the least squares analysis into a form where the

Table 3. Harmonic constituents required in analysis.

Over 27 days of data		13 to 26 days of data	
	Related		Related
Mean			
Mm		Mean	
Msf		Msf	
Q1		2Q1	
O1		O1	
M1		K_1	P_1
K1	π_1, P_1, ψ_1, ϕ_1	OO1	
J1		μ_2	
OO1		M_2	N_2
μ2		S_2	L_2, K_2
N2	ν_2, $2N_2$	$2SM_2$	
M2		M_3	
L2		SK_3	
S2	T_2, K_2	M_4	
2SM2		MS_4	
MO3		S_4	
M3		M_6	
MK3		$2MS_6$	
MN4		$2SM_6$	
M4			
SN4			
MS4			
2MN6			
M6			
MSN6			
2MS6			
2SM6			

constituent currents were resolved along the major and minor axes of the constituent tidal current ellipse would not help, since an assumption would still have to be made about the orientation of the ellipse of the related constituent. As well as this directional problem, in continental shelf seas the actual tidal dynamics are more complex than a simple progressive wave. Even this would not matter if it could be assumed that two related constituents had identical dynamics in a particular sea, with corresponding amphidromic points etc. But the subtleties of the dynamics within a sea, and the possibility of different modes of forcing at the continental edge for each constituent, mean that this assumption cannot be justified. To illustrate this it is instructive to compare M_2 and S_2 at station C_{73} in the middle of the Celtic Sea, where a tide gauge was situated. The ratio of the elevations is 2.96, of the north currents 1.78 and of the east currents 2.33. The corresponding differences in phase lag are 46, 39 and 51°. It will be seen later that the gross dynamics of these two constituents as

represented on a cotidal chart appear to be very similar, as one would expect in two constituents of fairly close frequency. However, if S_2 were related to M_2 in a current analysis on the basis of the elevation analysis, considerable errors would result. In shallower waters, where non-linearities enter the dynamics, the situation could be expected to be worse. Nonetheless, to ignore the related constituent altogether would produce even worse errors, and so the decision was made that where a constituent had to be related in an analysis the relations would be those obtained from a nearby port with a good year's analysis. For this purpose St Mary's, Fishguard, Holyhead, Hilbre Island, Douglas and Portpatrick, were used as indicated in Table 1. Since none of the related constituents thus obtained are actually used in the later sections of this paper, the exercise of relating constituents is performed simply to improve the accuracy of the least squares method in evaluating the more important constituents which are used. The results of Pugh & Vassie (1976), who had a year's analysis of current records at a site in the North Sea, indicate that relating currents to actual observations is slightly better than relating to the equilibrium elevations and is probably the best one can do. However, there is clearly scope for further study of this problem. The use of the equilibrium tide nodal corrections is also subject to similar criticism, but probably only where the dynamics are non-linear in very shallow water is there likely to be serious discrepancy. It is of course very necessary to include the nodal corrections since the data being used cover a period of seven years.

3 The tidal streams

Having obtained the harmonic constituents of the eastward and northward currents it was a simple matter of trigonometry to represent each tidal stream harmonic as the sum of two counter-rotating vectors from which the tidal stream ellipse could be constructed and plotted, and its sense of rotation deduced (see, e.g. Godin 1972, section 2.6). From computer plots of the tidal stream ellipse information it was possible to draw contours of ellipse amplitude, phase and direction. These are shown for M_2 in Fig. 2(a) and (b) and correspond to the average of upper and mid-depth meter records. The arrows indicate the direction of the ellipse maximum corresponding to the given phase. The overall picture is in general agreement with the previous charts by Bowden (1955) and Sager & Sammler (1975) although the detailed phase structure presented by the latter has not been identified with the available data. It must be borne in mind, however, that no attempt has been made to chart the tidal streams close inshore and around headlands where the topography may be expected to generate large tidal streams over short length scales. Throughout most of the Irish Sea the ellipses are very elongated, with the minor axis being less than 10 per cent of the major axis (Fig 2(c)). Exceptions are in the Celtic Sea towards the Irish and English coasts, station C_{75} having a ratio of 0.25, and in the northern Irish Sea off Morecombe Bay and the Cumbrian coast where the ratio reaches 0.6. The direction of rotation of the M_2 current vector is not uniform throughout the Irish Sea, and does not always appear to be the same for meters at different depths on the same rig. However, where the currents are strongly rectilinear the concept of the vector rotation has little significance, and its observation is more susceptible to errors. In the northern Irish Sea, east of the Isle of Man, the current vectors rotate counter-clockwise at every meter. The ellipse information is in general agreement with map 5 of Sager & Sammler (1975) apart from the Celtic Sea. Here, although the ellipse ratios reach 25 per cent, there is no coherent pattern nor is the sense of rotation consistent with the structure presented by Sager.

The S_2 currents are very similar to the M_2 currents in every aspect mentioned above and the dynamics of the two harmonics appear to be very similar, except when the relative

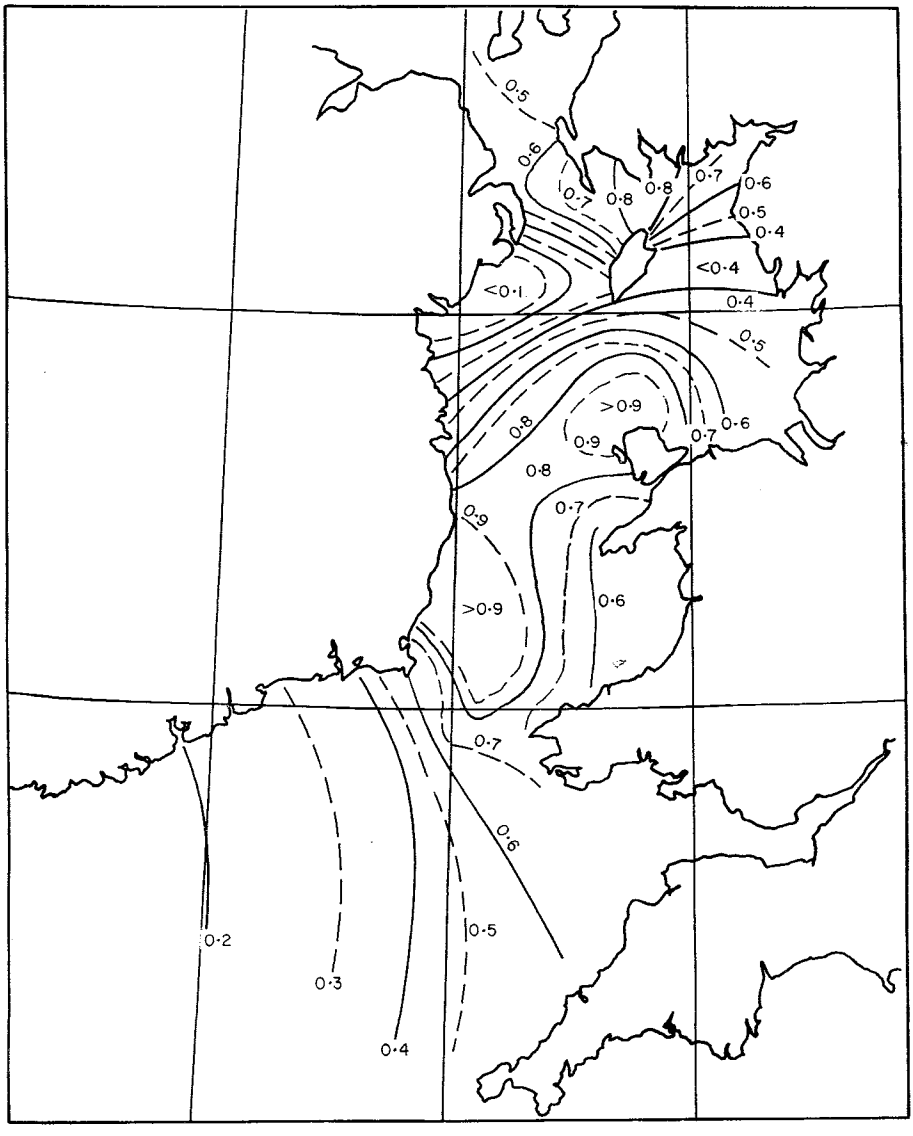

(a)

Figure 2. M_2 tidal streams. (a) Maximum velocity, m/s. (b) Phase and direction of maximum velocity. (c) Ellipse information. The number indicates the ratio of minor to major axes (per cent). a = anticlockwise rotation, c = clockwise, m = both senses of rotation found at different meters in the water column.

magnitudes of the ellipse maxima are compared in Fig. 3. Throughout the whole of the northern Irish Sea the ratio of S_2 to M_2 lies between 0.3 and 0.35, except for station F_{69} where the currents are extremely small in any case. There is, however, a definite decrease to a ratio of less than 0.2 towards Carnsore Point in St George's Channel and an increase westwards to a ratio of 0.5 in the Celtic Sea. There is no comparable effect in the coastal elevations, and whilst the phase difference between M_2 and S_2 currents appears to vary by a few degrees from station to station, there is no apparent pattern corresponding to the amplitude ratio. This anomaly may be due to the slightly different locations of M_2 and S_2

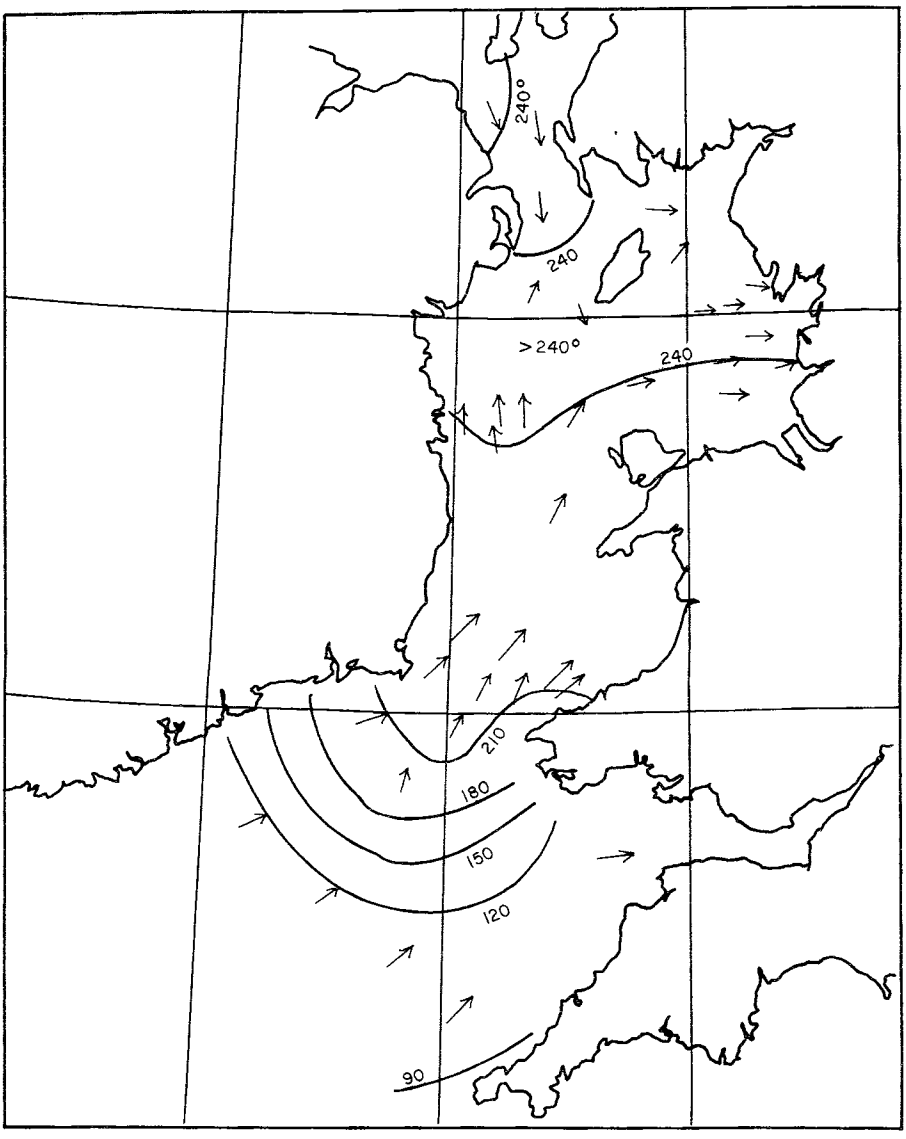

Figure 2(b)

current amphidromes, although it implies a significant difference between the semidiurnal dynamics at Spring and Neap tides, and its existence encourages further investigation of the tidal dynamics of the Celtic Sea out to the Shelf edge. The phenomenon may be connected with the dynamics of the response of the shelf tides to forcing by the deep ocean tides.

An accurate knowledge of S_2 as well as M_2 currents enables an evaluation of the different tidal mixing which might be expected at Spring and Neap tides. The parameter usually considered to control tidal mixing is U_0^3/h, where U_0 is the maximum tidal stream and h the depth. h may be considered to be independent of the Spring and Neap cycle, so that the plots of U_0^3 at Spring tide, mid-cycle and Neap tide in Fig. 4 indicate the fortnightly variation of tidal mixing which takes place. In particular it is of interest to note the excursion of a particular contour during the 14-day cycle. For the development of a seasonal

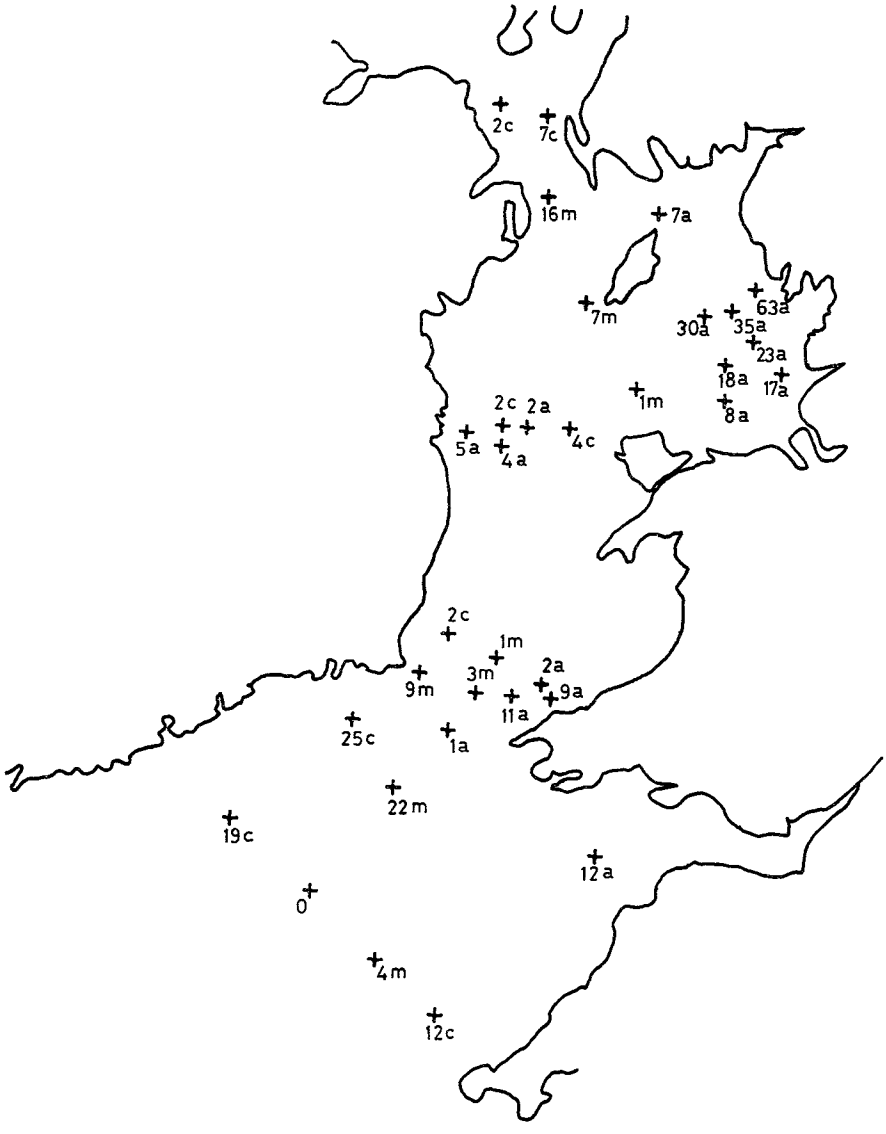

Figure 2 (c)

thermocline as suggested by Simpson *et al.* (1977), it will be seen that the extent of stratification to the west of the Isle of Man will show little variation over a Spring–Neap cycle, whereas in the Celtic Sea–St George's Channel the contours move as much as 100 km and this must affect the stable location of the summer front found in the zone between the stratified and well-mixed sea areas. Fig. 4 must, of course, be adjusted by the factor $1/h$ if it is to indicate an absolute measure of tidal mixing.

Although meters were placed at more than one depth on most rigs, the variations in water column depth between rigs, and a lack of uniformity between rigs of meter spacing within the column, make it difficult to draw other than general conclusions about the vertical structure of the tidal streams. For most rigs, if there was a bottom meter it was placed 5 m above the bed, and the current amplitudes there were 0.8 ± 0.1 of the currents in the middle

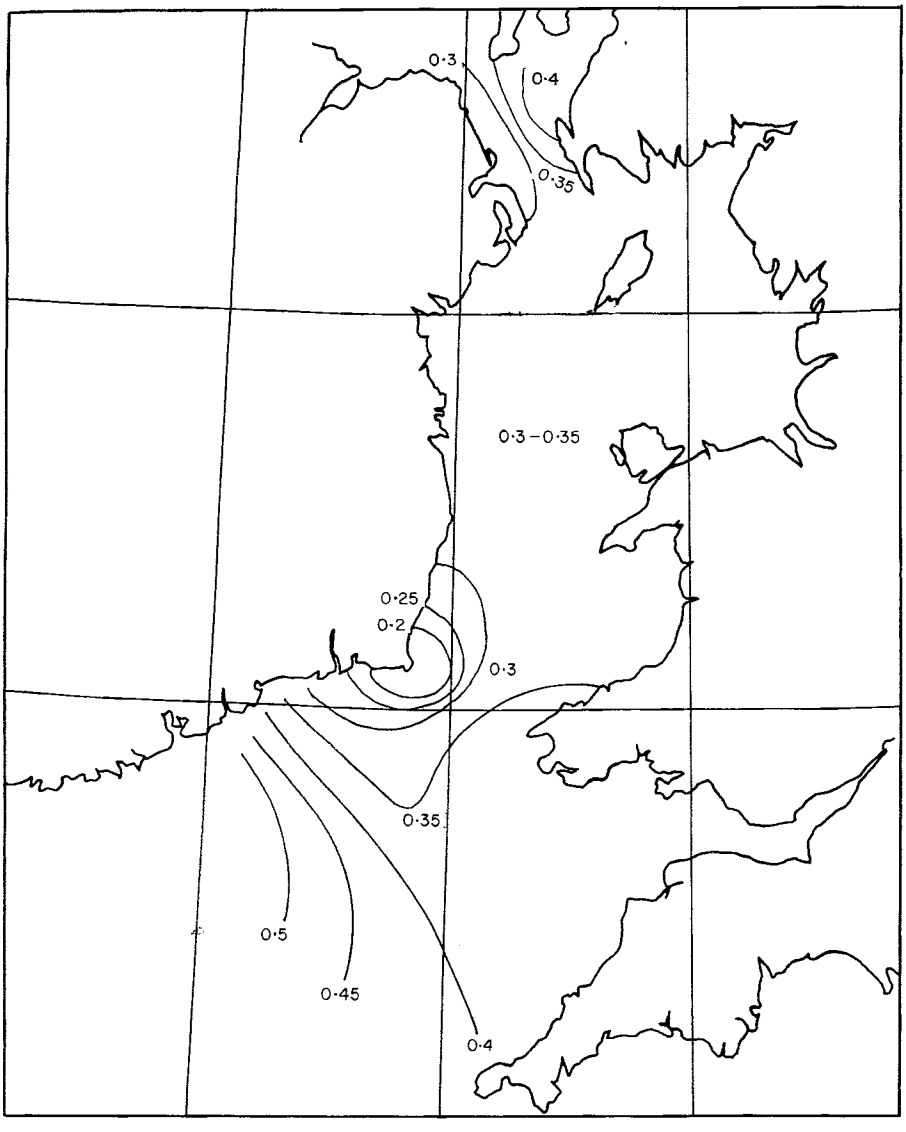

Figure 3. Ratio of maximum S_2 streams to maximum M_2 streams.

and upper parts of the water column where little variation with depth was noted. In general, also, the bottom currents tended to lag in phase behind the upper currents by about 10°, although this was less in the north-east off the Cumbrian and Lancashire coasts.

The currents for O_1 are shown in Fig. 5 and as expected are of a very different pattern from the semidiurnal currents, with a definite minimum value off Carnsore Point not far from the maximum currents of 4 cm/s in the centre of St George's Channel.

4 Cotidal maps

Following the approach of Proudman & Doodson (1924), cotidal maps can be constructed if the harmonic components of the surface slope are known at a number of stations through-

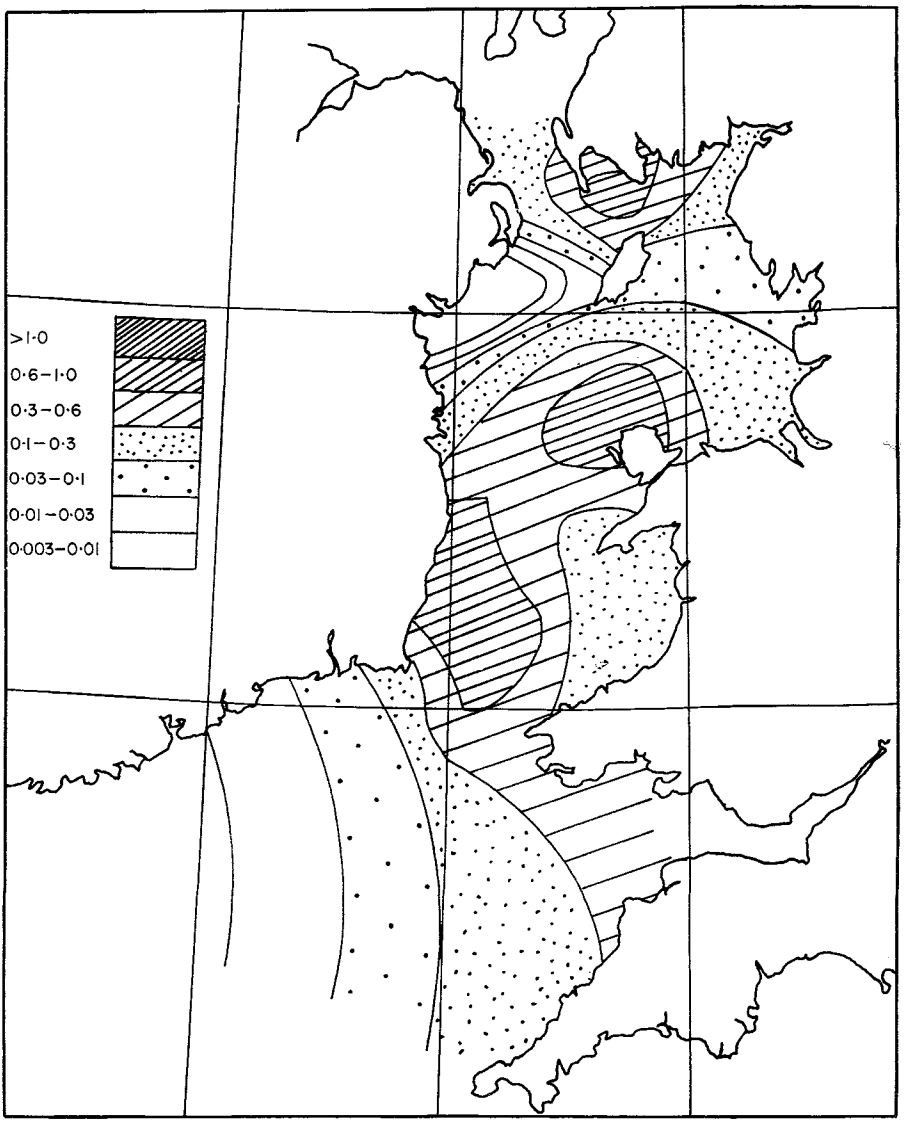

(a)

Figure 4. Contours of V^3 (m^3 s^{-3}). (a) M_2 alone. (b) $M_2 + S_2$ (Spring tides). (c) $M_2 - S_2$ (Neap tides).

out a particular sea area. Now the instantaneous surface slope is determined by the depth mean hydrodynamic equations of motion:

$$\frac{\partial \bar{u}}{\partial t} + u\frac{\overline{\partial u}}{\partial x} + v\frac{\overline{\partial u}}{\partial y} - f\bar{v} + g\frac{\partial \zeta}{\partial x} + \frac{k}{h}u_B\sqrt{u_B^2 + v_B^2} - \frac{\partial \zeta_E}{\partial x} = 0$$

$$\frac{\partial \bar{v}}{\partial t} + u\frac{\overline{\partial v}}{\partial x} + v\frac{\overline{\partial v}}{\partial y} + f\bar{u} + g\frac{\partial \zeta}{\partial y} + \frac{k}{h}v_B\sqrt{u_B^2 + v_B^2} - \frac{\partial \zeta_E}{\partial y} = 0$$

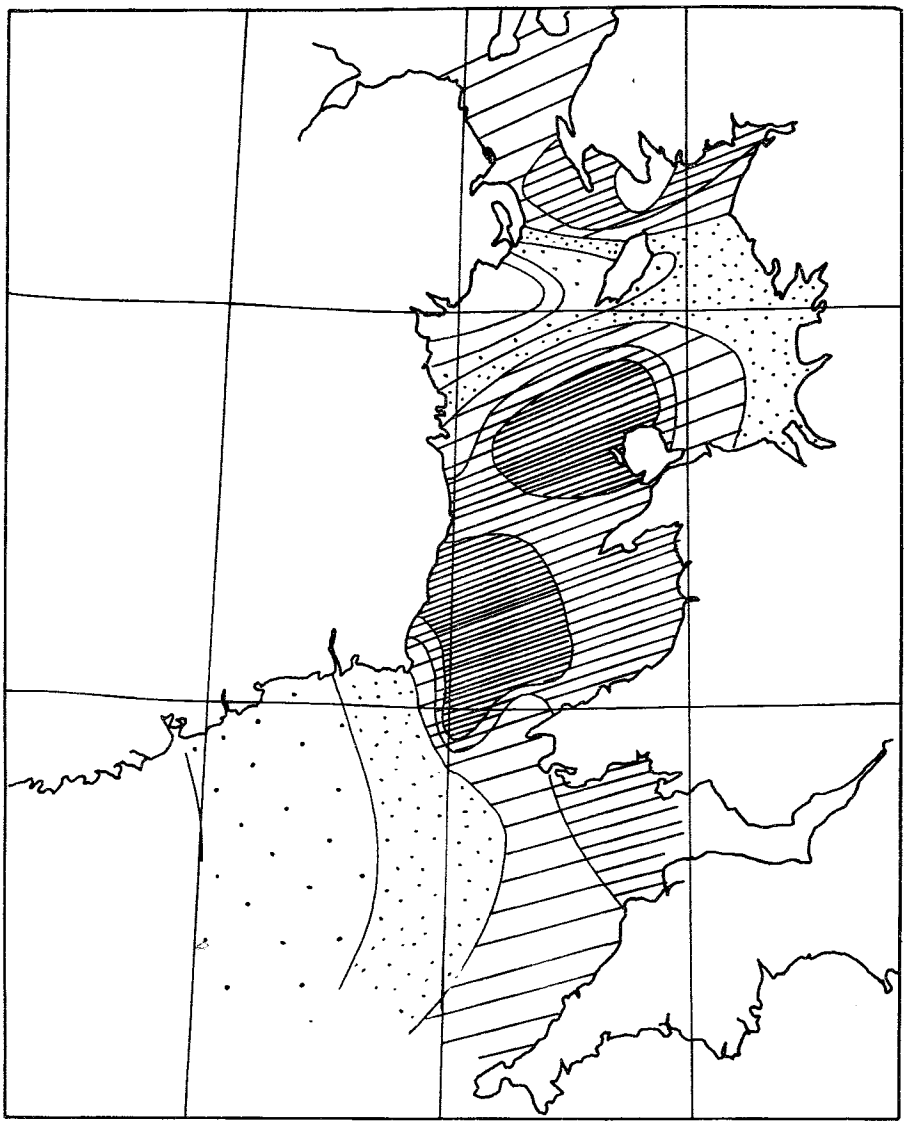

Figure 4 (b)

where u, v are velocities in the eastward (x) and northward (y) directions, and an overbar denotes a depth mean, e.g.

$$\bar{u} = \frac{1}{h}\int_{-h}^{0} u\,dz,$$

where h is the sea depth below mean sea-level and the effect of finite amplitude has been ignored, assuming $\zeta \ll h$. ζ is the height of the sea surface above a geopotential datum, ζ_E is the equilibrium tidal height adjusted to include the effect of Earth tides, and k is the coefficient of bottom friction, relating the bottom stress to the velocity u_B, v_B at a particular height above the sea-bed. A quadratic friction has been assumed, and wind stress

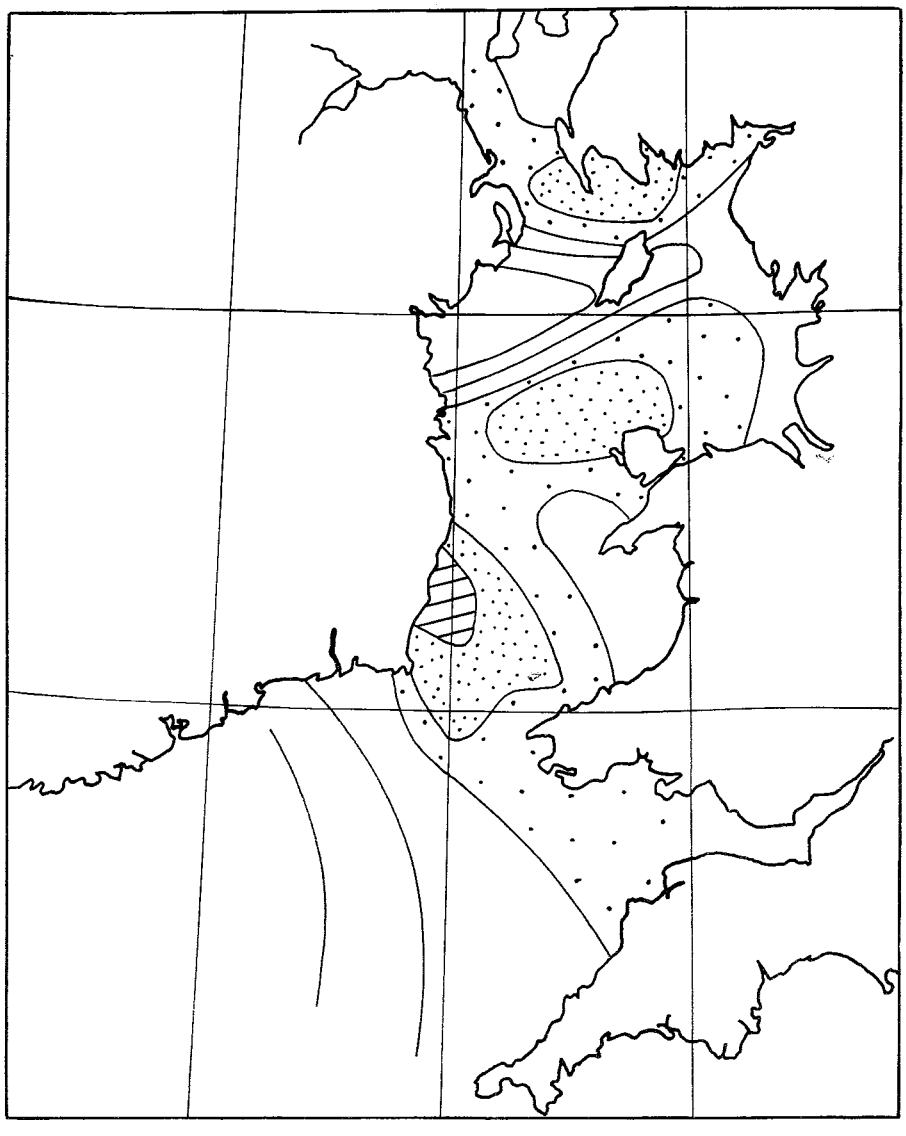

Figure 4 (c)

has been neglected, in anticipation of the following paragraph, since it will not contribute to the dynamics of particular tidal harmonics. The neglect of finite amplitude in the depth means, and in the friction terms, is necessitated by the lack of simultaneous elevation time series at all the current meter stations. It is justified in that $|\zeta/h| < 0.05$ over most of the Irish Sea except in Liverpool Bay and off the Lancashire coast. This is the only area where the errors in ignoring finite depth may be larger than those which arise in any case from the poor determination of the true vertical velocity structure and hence the true depth mean, and the somewhat arbitrary choice of k, u_b and v_b (see below).

We are interested in particular harmonics of the time series representation of surface slope. Therefore we assume that terms involving u and ζ can be represented as the sum of

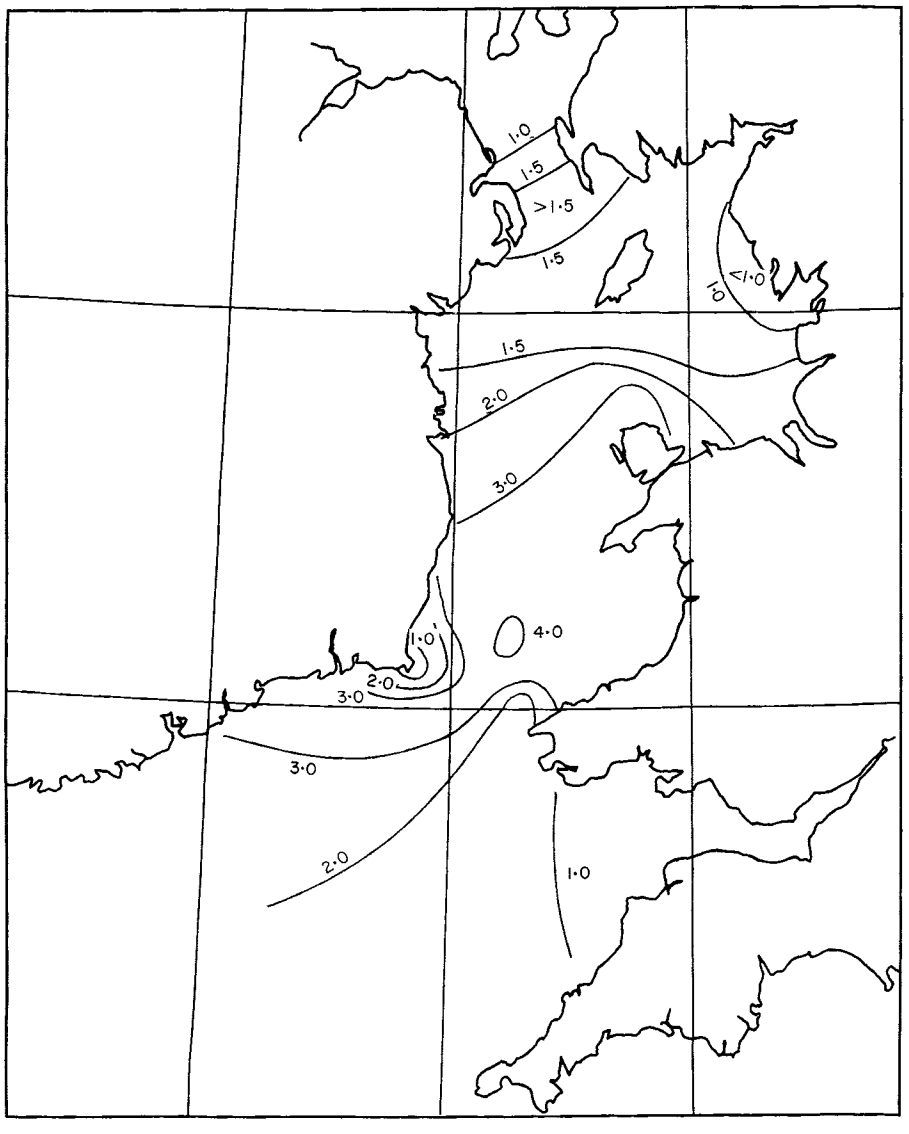

Figure 5. O_1 maximum tidal streams (cm/s).

tidal harmonics, i.e.

$$\bar{u} = \sum_{n=1}^{N_1} u_{nc} \cos \sigma_n t + u_{ns} \sin \sigma_n t$$

$$\bar{v} = \sum_{n=1}^{N_1} v_{nc} \cos \sigma_n t + v_{ns} \sin \sigma_n t$$

$$\zeta = \sum_{n=1}^{N_1} \zeta_{nc} \cos \sigma_n t + \zeta_{ns} \sin \sigma_n t = \sum_{n=1}^{N_1} \zeta_{on} \cos (\sigma_n t - g_n).$$

The values of u_{nc}, u_{ns}, v_{nc} and v_{ns} were obtained at each station as the average over the depth of the harmonic constituents of east and north currents from each meter at that

station. The local effect of the tide generating potential was ignored, i.e. $\nabla\zeta_E$ was neglected compared with $\nabla\zeta$. Then if the following tidal harmonic expansions of the remaining terms in the equation of motion are assumed:

$$\overline{u\frac{\partial u}{\partial x}} + \overline{v\frac{\partial u}{\partial y}} = \sum_{n=1}^{N_2} a_{nc}\cos\sigma_n t + a_{ns}\sin\sigma_n t$$

$$\overline{u\frac{\partial v}{\partial x}} + \overline{v\frac{\partial v}{\partial y}} = \sum_{n=1}^{N_2} c_{nc}\cos\sigma_n t + c_{ns}\sin\sigma_n t$$

$$\frac{k}{h}u_B\sqrt{u_B^2 + v_B^2} = \sum_{n=1}^{N_3} b_{nc}\cos\sigma_n t + b_{ns}\sin\sigma_n t$$

$$\frac{k}{h}v_B\sqrt{u_B^2 + v_B^2} = \sum_{n=1}^{N_3} d_{nc}\cos\sigma_n t + d_{ns}\sin\sigma_n t$$

then for a particular frequency σ_n, the equations of motion simplify to

$$-g\frac{\partial\zeta_{nc}}{\partial x} = \sigma_n u_{ns} - fv_{nc} + a_{nc} + b_{nc}$$

$$-g\frac{\partial\zeta_{ns}}{\partial x} = -\sigma_n u_{nc} - fv_{ns} + a_{ns} + b_{ns}$$

$$-g\frac{\partial\zeta_{nc}}{\partial y} = \sigma_n v_{ns} + fu_{nc} + c_{nc} + d_{nc}$$

$$-g\frac{\partial\zeta_{ns}}{\partial y} = -\sigma_n v_{nc} + fu_{ns} + c_{ns} + d_{ns}.$$

In this way the instantaneous acceleration term (e.g. $\sigma_n u_{ns}$) can be obtained from the velocity harmonics, rather than by analysing a time series of acceleration constructed by differencing the original current meter rotor counts which introduces considerable digital error and produces a very spiky time series. The Coriolis term is straightforward. The remaining two terms in each slope equation are obtained by constructing a time series of hourly values of the advective term and the bottom stress term from the instantaneous velocities as recorded at each rig, and reducing these by harmonic analysis to their tidal constituents. In practice the constituents required in the analysis were the same as for the velocities (see Table 3), including constituents related by local elevations (i.e. $N_1 = N_2 = N_3$). The bottom stress time series was constructed using $k = 0.002$, u_B and v_B being the hourly values of east and north currents at the lowest meter available on a particular rig, in most cases at 5 m from the bottom. This clearly takes no account of the effect on the bottom friction of any variation of velocity profile from rig to rig, but it does at least enable the gross effects of friction to be taken into account in the slope equation. The construction of the advective term time series was only possible when a suitable array of current meter stations had been laid at one time, thus permitting hourly values of the instantaneous spatial velocity gradients to be determined. To simplify the data processing, terms such as $\bar{u}(\partial\bar{u}/\partial x)$ were evaluated rather than $\overline{u(\partial u/\partial x)}$, since within an array of stations different rigs had meters at different levels. The resulting error should be small compared with that resulting from the assumption that a local velocity gradient can be obtained from differencing the velocity at stations up to 100 km apart. For many of the rigs, it was impossible to construct

Table 4. Station groups where advective terms were constructed.

A_{73}, C_{73}, D_{73}, G_{73}, H_{73}.

C_{74}, D_{74}, E_{74}, J_{74}.

GS_{72}, G_{72}, GE_{72}, M_{72}.

A_{72}, B_{72}, C_{72}, D_{72}.

an advective term, and this had to be omitted from the evaluation of the slope harmonics at each station. The stations where advective terms could be constructed are indicated in Table 4.

It is interesting to compare the typical magnitude of the different terms in the slope equations, at different locations in the Irish Sea. Table 5 indicates the amplitude of each term at the principal constituent within each tidal species from one to four cycles per day. The locations are in the Celtic Sea, in St George's Channel and between Holyhead and Dublin. The contributing terms are given as east and north components, the value of the resulting slope is the value in the direction of maximum slope. In all cases the acceleration and Coriolis terms are the largest, and in some cases the non-linear terms can be neglected compared with the resulting value of the slope. However, the contribution of bottom friction is of the order of 10 per cent for all the harmonics at each of the stations considered. It is worth noting in general that, at a particular station, the magnitude of the bottom stress term for each harmonic varies approximately in direct proportion to the current magnitudes for each harmonic, whereas between stations the friction, for M_2 at least, has a higher-order dependence on velocity. This bears out the results of le Provost (1973a, b) which show how the background of strong semidiurnal currents enhances the friction forces at other frequencies above the quadratic values which would be expected in the absence of the background. This is a weak interaction compared with the strong interactions which occur at the sixth and tenth diurnal species and can be expected to be the dominant driving term at these frequencies. At the third diurnal and quarter-diurnal frequencies the friction terms are dissipative rather than driving, but are nonetheless significant. We must conclude

Table 5. Typical magnitude of terms in the slope equation. Units of slope × 10^5 (i.e. mm/km).

Station	Harmonic	Max. slope	Instantaneous accln. $\frac{\partial u}{g}$ East	Instantaneous accln. $\frac{\partial v}{g}$ North	Coriolis accln. $\frac{fv}{g}$ East	Coriolis accln. $\frac{fu}{g}$ North	Advective term $\frac{a}{g}$ East	Advective term $\frac{c}{g}$ North	Bottom stress $\frac{b}{g}$ East	Bottom stress $\frac{d}{g}$ North
D_{73}	O_1	0.111	0.085	0.055	0.092	0.141	0.0028	0.0024	0.008	0.0056
	M_2	4.01	4.08	2.74	2.27	3.38	0.0049	0.0048	0.158	0.076
	M_3	0.073	0.064	0.056	0.031	0.035	0.0015	0.0019	0.0012	0.0008
	M_4	0.094	0.145	0.423	0.175	0.060	0.049	0.085	0.0038	0.0066
D_{74}	O_1	0.266	0.198	0.244	0.407	0.330	0.042	0.012	0.022	0.090
	M_2	11.4	9.17	10.50	8.69	7.59	0.100	0.238	0.074	1.47
	M_3	0.112	0.089	0.223	0.123	0.049	0.003	0.037	0.008	0.019
	M_4	0.782	0.978	0.497	0.206	0.405	0.584	0.514	0.012	0.085
GS_{72}	O_1	0.212	0.041	0.173	0.289	0.068	0.032	0.014	0.013	0.066
	M_2	10.8	1.82	10.31	8.53	1.51	0.20	0.21	0.195	1.31
	M_3	0.043	0.058	0.036	0.020	0.032	0.023	0.005	0.007	0.005
	M_4	0.916	0.894	0.921	0.381	0.370	0.196	0.539	0.043	0.072

that the inclusion of the friction terms at all stations is necessary for the accurate construction of cotidal charts for all frequencies.

By contrast the advective terms can be neglected for the diurnal and semidiurnal frequencies without serious loss of accuracy, although they are not so small that their inclusion is not worthwhile where possible. For M_4 the advective terms are of the same magnitude as the slope, and their neglect at certain stations will render meaningless the interpretation of the currents in terms of surface slope. Advective terms are expected to be large at M_4 since terms in u^2 are involved and if $u = A \cos \sigma t$, σ being the M_2 frequency, then the expansion of u^2 involves a mean and cos 2 σt terms. We would expect also a mean surface slope to be set up where the M_4 slopes are large, which through the fortnightly Spring/Neap modulations will drive the non-astronomical contribution to the fortnightly period tides. The M_3 advective terms must be treated with care. Because the M_3 frequency cannot be produced by combinations of fundamental tidal frequencies, it must be present only through astronomical forcing in the deep ocean. We would therefore expect the advective terms to be very small. Examination of several stations shows the M_3 advective terms to be an order of magnitude smaller than other third diurnal harmonics in the analyses such as MK_3 and SK_3 which are true interaction frequencies. There are instances however where this is not the case, as for D_{74} and GS_{72} east. These spurious larger values are probably due to lack of resolution between M_3 and other spectrally adjacent harmonics and must corrupt the M_3 slope value.

Having obtained values of the slope for each harmonic in the east and north directions, the expressions of Proudman & Doodson were used to deduce the directions of cotidal and corange lines at each station, i.e. if the cotidal line for a tidal frequency σ_n makes an angle ψ_n with the x axis,

$$\tan \psi_n = -\frac{\zeta_{nc}(\partial\zeta_{ns}/\partial x) - \zeta_{ns}(\partial\zeta_{nc}/\partial x)}{\zeta_{nc}(\partial\zeta_{ns}/\partial y) - \zeta_{ns}(\partial\zeta_{nc}/\partial y)}$$

and if n is the normal direction to the cotidal line, the gradient of phase is

$$\frac{\partial g_n}{\partial n} = \frac{1}{\zeta_{on}^2}\left\{\left(\zeta_{nc}\frac{\partial\zeta_{ns}}{\partial x} - \zeta_{ns}\frac{\partial\zeta_{nc}}{\partial x}\right)^2 + \left(\zeta_{nc}\frac{\partial\zeta_{ns}}{\partial y} - \zeta_{ns}\frac{\partial\zeta_{nc}}{\partial y}\right)^2\right\}^{1/2}.$$

Similarly for the corange line:

$$\tan \psi_n' = -\frac{\zeta_{nc}(\partial\zeta_{nc}/\partial x) + \zeta_{ns}(\partial\zeta_{ns}/\partial x)}{\zeta_{nc}(\partial\zeta_{nc}/\partial y) + \zeta_{ns}(\partial\zeta_{ns}/\partial y)}$$

and

$$\frac{\partial\zeta_{on}}{\partial n'} = \frac{1}{\zeta_{on}}\left\{\left(\zeta_{nc}\frac{\partial\zeta_{nc}}{\partial x} + \zeta_{ns}\frac{\partial\zeta_{ns}}{\partial x}\right)^2 + \left(\zeta_{nc}\frac{\partial\zeta_{nc}}{\partial y} + \zeta_{ns}\frac{\partial\zeta_{ns}}{\partial y}\right)^2\right\}^{1/2}.$$

ψ amd ψ' can therefore be determined from the calculated components of slope, and the phase of the elevation constituent at each station. Now g_n is not known by observation offshore except at the three stations where an offshore tide gauge was located. At all the other stations ζ_{nc} and ζ_{ns} were estimated by linear interpolation between coastal and offshore tide gauges. This clearly introduces uncertainty into the evaluation of ψ and ψ'. To assist in the drawing of the cotidal maps, it was useful to have a numerical value of this error,

obtained by computing

$$\frac{\partial \psi_n}{\partial g_n} = \cos^2 \psi_n \frac{(\partial \zeta_{nc}/\partial y)(\partial \zeta_{ns}/\partial x) - (\partial \zeta_{nc}/\partial x)(\partial \zeta_{ns}/\partial y)}{[(\partial \zeta_{ns}/\partial y)\cos g_n - (\partial \zeta_{nc}/\partial y)\sin g_n]^2}$$

$$\frac{\partial \psi_n'}{\partial g_n} = \cos^2 \psi_n' \frac{(\partial \zeta_{nc}/\partial x)(\partial \zeta_{ns}/\partial y) - (\partial \zeta_{ns}/\partial x)(\partial \zeta_{nc}/\partial y)}{[(\partial \zeta_{nc}/\partial y)\cos g_n + (\partial \zeta_{ns}/\partial y)\sin g_n]^2}.$$

For a particular frequency, given the harmonic constants of each term in the slope equation at every station, the above expressions were evaluated and automatically plotted by a computer onto an outline map of the Irish Sea, in the form indicated in Fig. 6. The local direction of the cotidal line is indicated by the solid line, and the spacing between cotidal lines by the dashed line at right angles, while the number indicates the estimate of

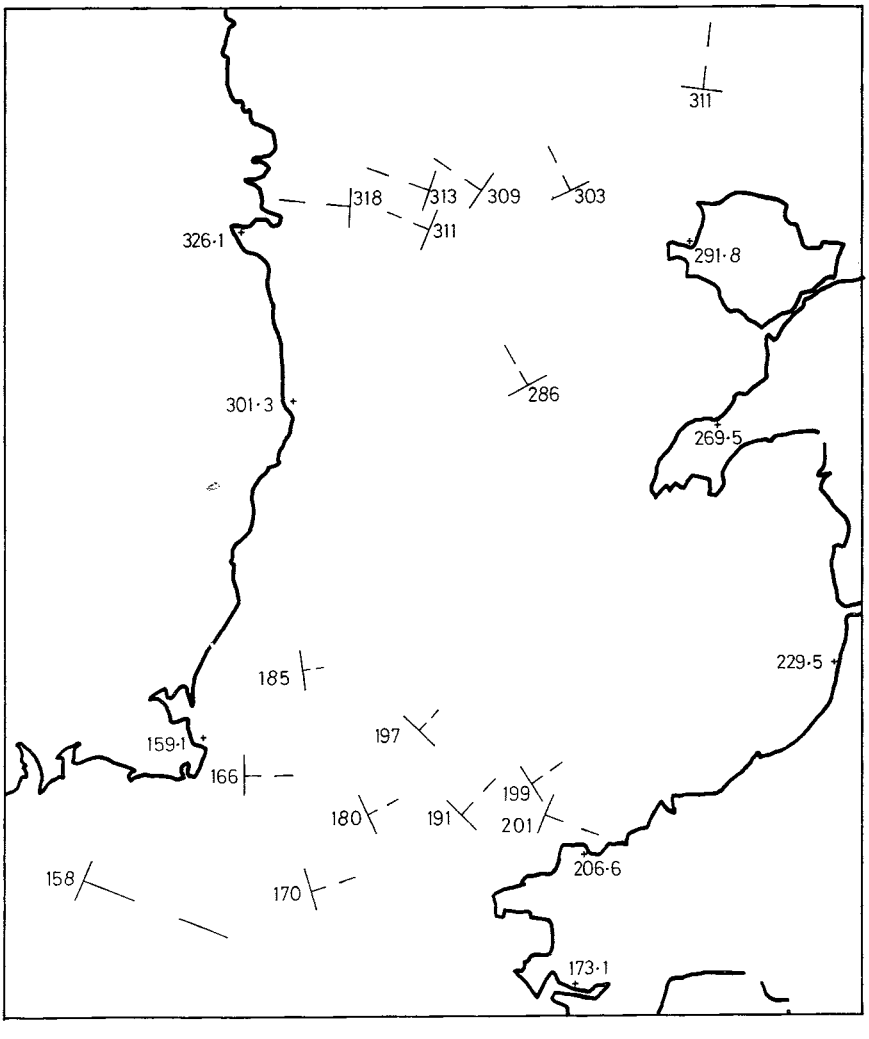

Figure 6. Typical computer plot from which the cotidal maps were drawn. This shows the phase plot for M_2.

phase at that station. Similar plots were produced for the corange lines. Then followed the subjective exercise of drawing in the cotidal lines, using the coastal and offshore tide gauge data as fixed references (except where there was ground for doubting their validity in the case of very old, or short-span data). The value of phase estimated at other offshore locations was used as a guide only, and where the estimate was clearly wrong, the values of $\partial\psi_n/\partial g_n$ were used to recalculate the appropriate cotidal line direction. The technique used by Proudman & Doodson of interpolating for the phase along lines of current stations, using the known value of surface slope, was not adopted, both because the distribution of available current meter stations did not lend itself to the method and also because it could not be easily included in the automatic data processing sequence necessary to handle the data efficiently. Instead, when the maps had been drawn once, the whole process was repeated, using offshore elevation data obtained from the stage one maps instead of by interpolation from the coast. Small differences could be noted between the stage one and two maps, but there were no alterations significant enough to warrant a further iteration to a stage three map.

Cotidal maps were drawn for M_2, S_2, O_1, K_1, M_3 and M_4, and these are found in Figs 7 to 12. Attempts were made to plot a map for M_6, but no coherent tidal pattern emerged from the available data, due in part to noise in the data corrupting the harmonic signals, but probably due mostly to the fact that the M_6 dynamics depend on local frictional forcing and must vary on a typical length scale smaller than the typical spacing between the stations. The comments below concerning M_4 are also appropriate to M_6. Since the cotidal maps are intended to represent our most accurate knowledge of the tidal regime in the Irish Sea, based on the most reliable and recent tidal stream observations available, every effort was made to depend entirely on the observed data when drawing the maps. Inevitably, however, subjective judgement was involved and the following comments should be noted if the maps are used as a basis for further work.

In general there was little ambiguity in the regions well covered by stations, where any error in a particular station was apparent by comparison with the trend dictated by all the other stations in the vicinity. Conversely, lines had to be drawn entirely subjectively in areas with a paucity of stations, notably the region off the coast of Wicklow across to Cardigan Bay, from the west of the Isle of Man to the North Channel, off St Bees head to the Solway Firth and at the mouth of the Bristol Channel. Nonetheless, for the diurnal and semidiurnal constituents it is considered that there can be no possibility of more than minor variations from the lines as drawn, on the assumption that the dynamics of these constituents are dominated by a long wave-like mechanism, with energy flowing in from the open boundaries and being dissipated but not generated in the Irish Sea (i.e. one would not expect the lines to be sharply curved, nor for structures to be present on a scale small enough to be lost in the ambiguous areas). Comparison between the maps and some of the less reliable coastal observations implies errors in the latter. All the reliable coastal data are consistent except for Rosslare harbour. It was consistently difficult to fit the phase of Rosslare into the pattern dictated by the good coverage of stations in St George's Channel, linked to the very reliable Fishguard tide gauge harmonics, the tendency being for the tide gauge to lag several degrees behind the phase required by the map. There is no reason to question the Rosslare analysis which is based on 319 days of data from 1972/73 and the discrepancy is probably due to local effects in Rosslare harbour and around Carnsore Point. This uncertainty is unfortunately placed for the semidiurnal tides because the degenerate amphidromic system lies to the north of Rosslare and cannot be defined precisely because there are neither current meter stations offshore, nor tide gauge records on the coast between Rosslare and Wicklow. It is also a reminder that care must be taken when assuming that a coastal gauge is

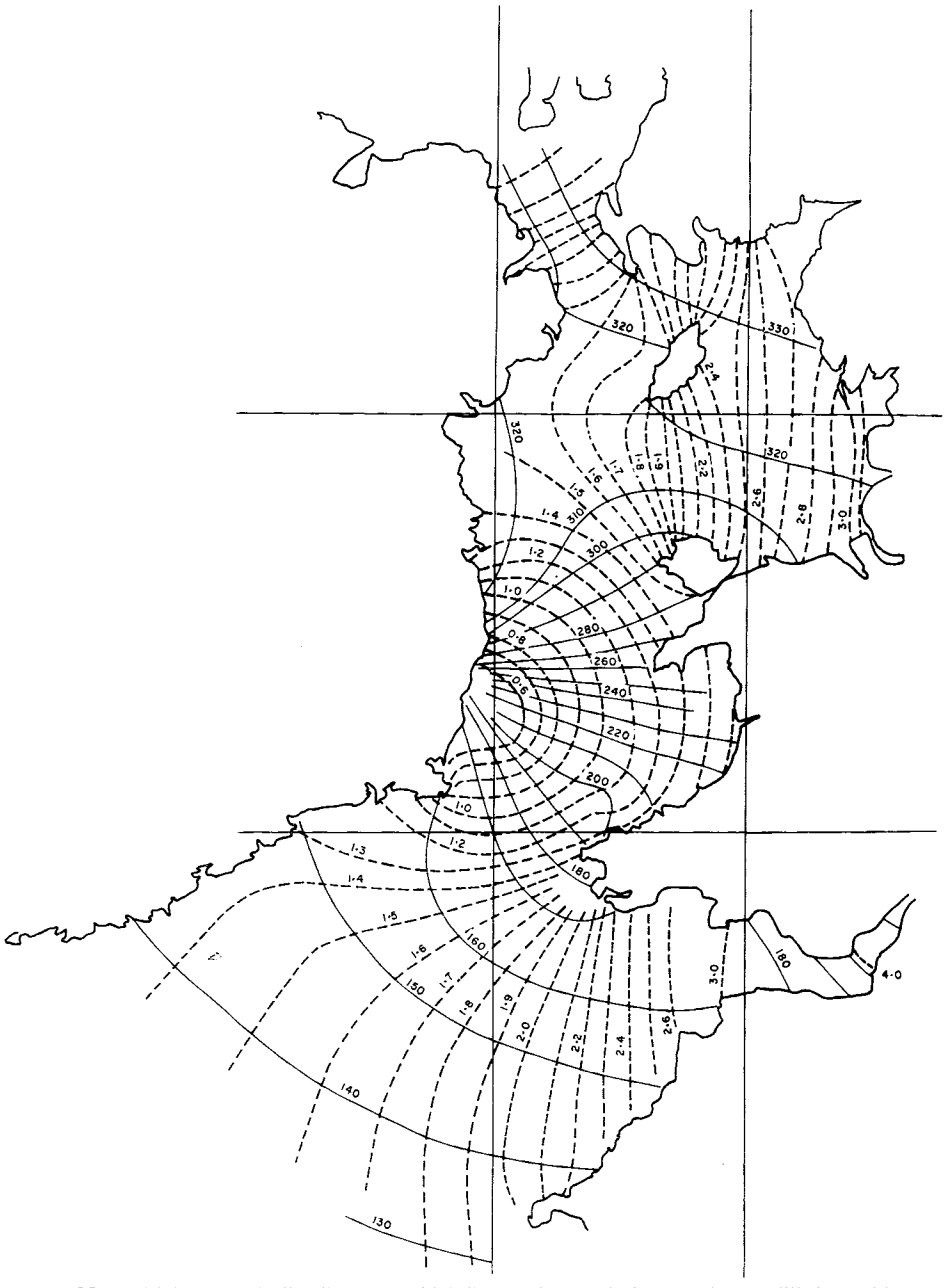

Figure 7. M_2 cotidal maps (solid lines – cotidal lines, phase relative to the equilibrium tide at the Greenwich meridian, dashed lines – coamplitude lines in m).

representative of offshore elevations, even for frequencies as low as the diurnal and semi-diurnal.

Although M_3 is unimportant in the Irish Sea, and indeed it is unlikely that a cotidal map for it exists for any other sea, it was plotted out of interest to examine the typical response of the sea to third diurnal forcing. The M_3 data are by no means as reliable as the semi-diurnal and diurnal data, the amplitudes of M_3 currents being very small, but surprisingly

little difficulty was experienced in producing a cotidal map since most of the stations gave line directions and spacings which were mutually consistent. This is probably because there is no generation of M_3 by non-linear interactions and it propagates through the region as a free wave. Even so, the degenerate amphidrome placed in the Isle of Man was not dictated by the offshore stations which are lacking in that area, but is a subjective feature which seemed to be required by the coastal observations and the pattern in the eastern Irish Sea. Its existence needs further confirmation.

Although M_4 current amplitudes were an order of magnitude greater than the M_3 currents, and therefore likely to be less noisy, the line directions and spacings were not so consistent, and the map was consequently harder to draw with confidence in its accuracy. In the areas well covered by stations a clear trend for the cotidal pattern was apparent, which agreed in general with coastal elevation data, but within the trend individual stations often indicated line directions 10° or so different from the trend. This could either indicate a small-scale pattern structure, or else errors in the data. The latter was assumed, and the lines were drawn smoothly as for the lower frequency maps. Errors could arise from inaccurate estimates of the current harmonics, due to both rig-induced quarter-diurnal noise in the record, and inadequate resolution from a short data span, of M_4 from the other quarter-diurnal harmonics present in the time series. They would also be the result of inaccurate evaluation of the non-linear terms in the slope equations, both by construction of the advective terms from unrealistic velocity gradients, and again from inadequate resolution of M_4 in the harmonic analysis of the advective time series. It is interesting to note that the stations where the advective term was not available usually predicted the line directions within the general trend, but tended to show most discrepancy in the gradients (i.e. the line spacing). The presence of small-scale structure cannot be ruled out however, because much of the quarter-diurnal energy is generated within the area, and the system cannot be conceived adequately in the terms of progressive and standing waves by which the M_2 chart is interpreted. The cotidal and corange lines could therefore be capable of much greater complexity than we are accustomed to expect from the lower frequency cotidal maps. The problem of drawing the M_4 chart was compounded by the local inconsistencies of coastal data, apparent in the areas where the offshore data indicated a fairly consistent picture. These inconsistencies could be due to the limitations of harmonic analysis for short coastal records, but may well be the results of a very local non-linear interaction within a bay or estuary. This is a reminder that M_4 will vary most rapidly in the shallowest areas where its generation is strongest, and so small-scale structure is very likely close inshore. The map as drawn can only be considered to represent the offshore variation of M_4 and it would be erroneous to extrapolate the lines right up to the coastline. For this reason the coastal observations cannot be confidently used in filling the gaps left by the current meter stations. In particular the regime in the north-west around the Isle of Man and into the North Channel is little more than guesswork. It could be that the amphidrome should be located in the Isle of Man, or does not exist at all, and its existence needs confirmation by further observations.

When the M_2 cotidal map in Fig. 7 is compared with the early Admiralty chart No. 301 based on Doodson & Corkan (1932), the more recent Admiralty chart No. 5058 (which is drawn in terms of mean high water interval and mean Spring range) and the German chart of 1942 (Marineobservatorium Wilhelmshaven 1942), the same general features are present in them all; the degenerate amphidrome at the Wicklow–Wexford coast and the standing wave in the northern Irish Sea. Close inspection of the cotidal lines reveals that the map presented here agrees most nearly with Admiralty chart 301, the phases being the same to within about a degree in most places, apart from a slight shift southward of the degenerate amphidrome and a local speedup of the tidal wave off Fishguard in this chart. However, the Admiralty

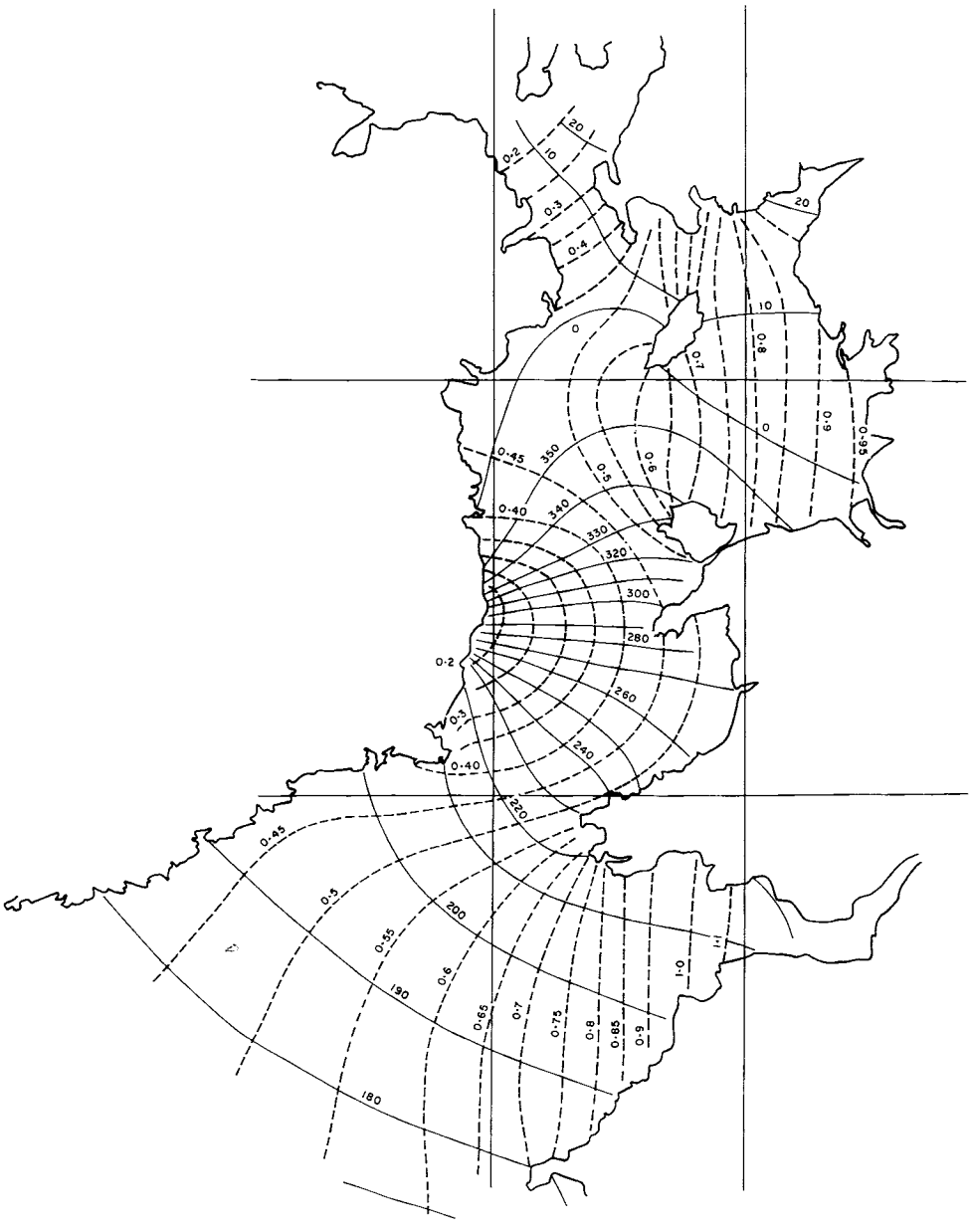

Figure 8. S_2 cotidal map.

chart 5058 and the early German chart show the cotidal lines progressing with a convex shape through the Celtic Sea compared with the concave shape of Doodson and this paper. Consequently the phase indicated by the German charts is 15–20° in advance of that observed at station C_{73} in the centre of the Celtic Sea, i.e. an error of over 30 min early. This advance in phase also requires the pattern of lines through St George's Channel to be different. If it is assumed that the $M_2 : S_2$ elevation ratio is 3:1, chart 5058 can be interpreted for the M_2 range and then comparison between the ranges in the different charts again shows good agreement in the northern Irish Sea. In the Celtic Sea, the German chart shows a low

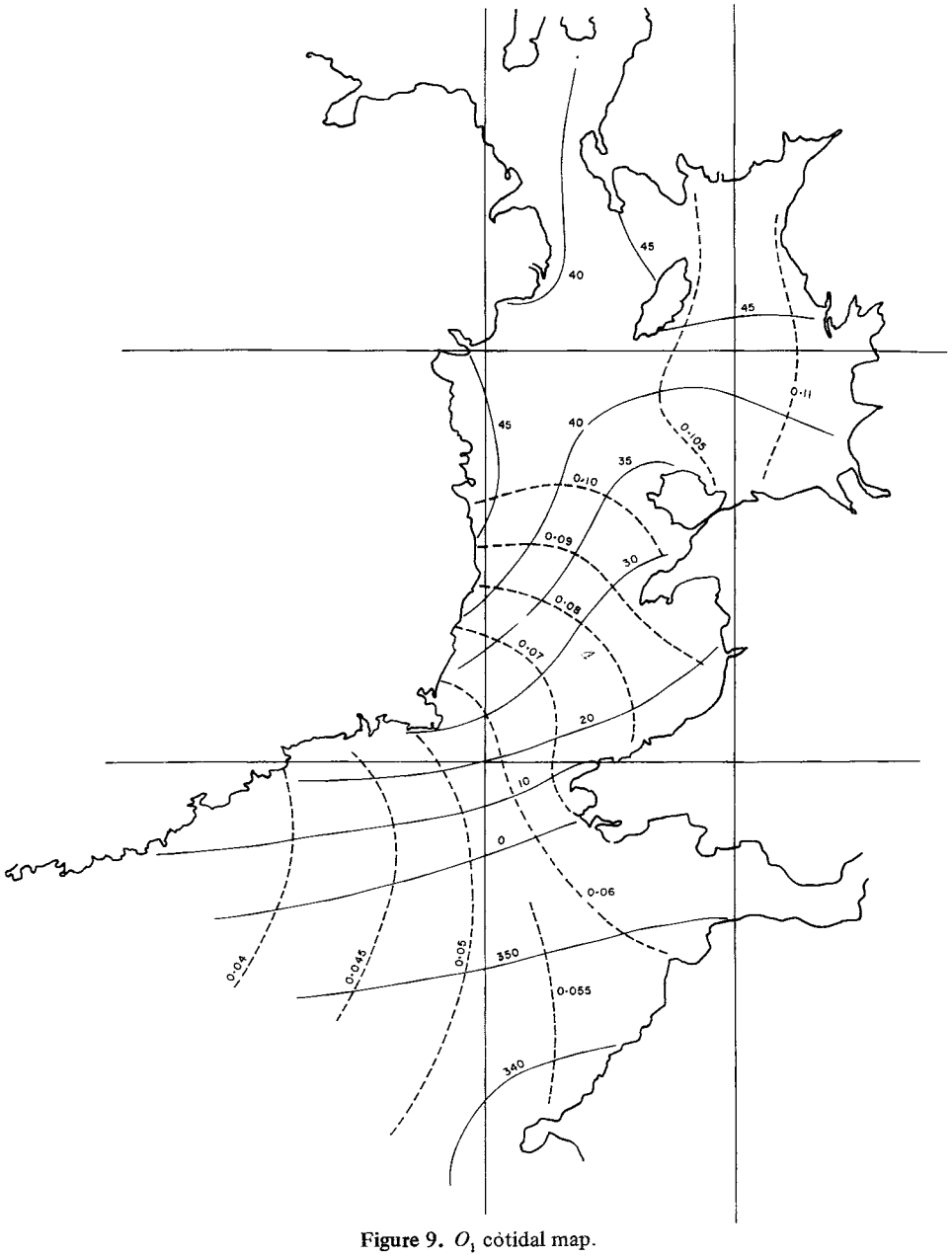

Figure 9. O_1 cotidal map.

amplitude feature penetrating up towards St George's channel which is not supported by the modern data. This is reflected to a lesser extent in chart 5058 which indicates a range some 60 cm less than the data suggests between longitudes 6 and 7° W at the mouth of the Bristol Channel. Chart 301 tends to agree better with the chart presented here, but neither of the Admiralty charts gives enough detail off the south Irish coast for a thorough comparison to be made.

The other cotidal maps, Figs 8–12, can be compared with the German 1942 atlas. The S_2 maps are similar to the corresponding M_2 maps in each case and the same comments are

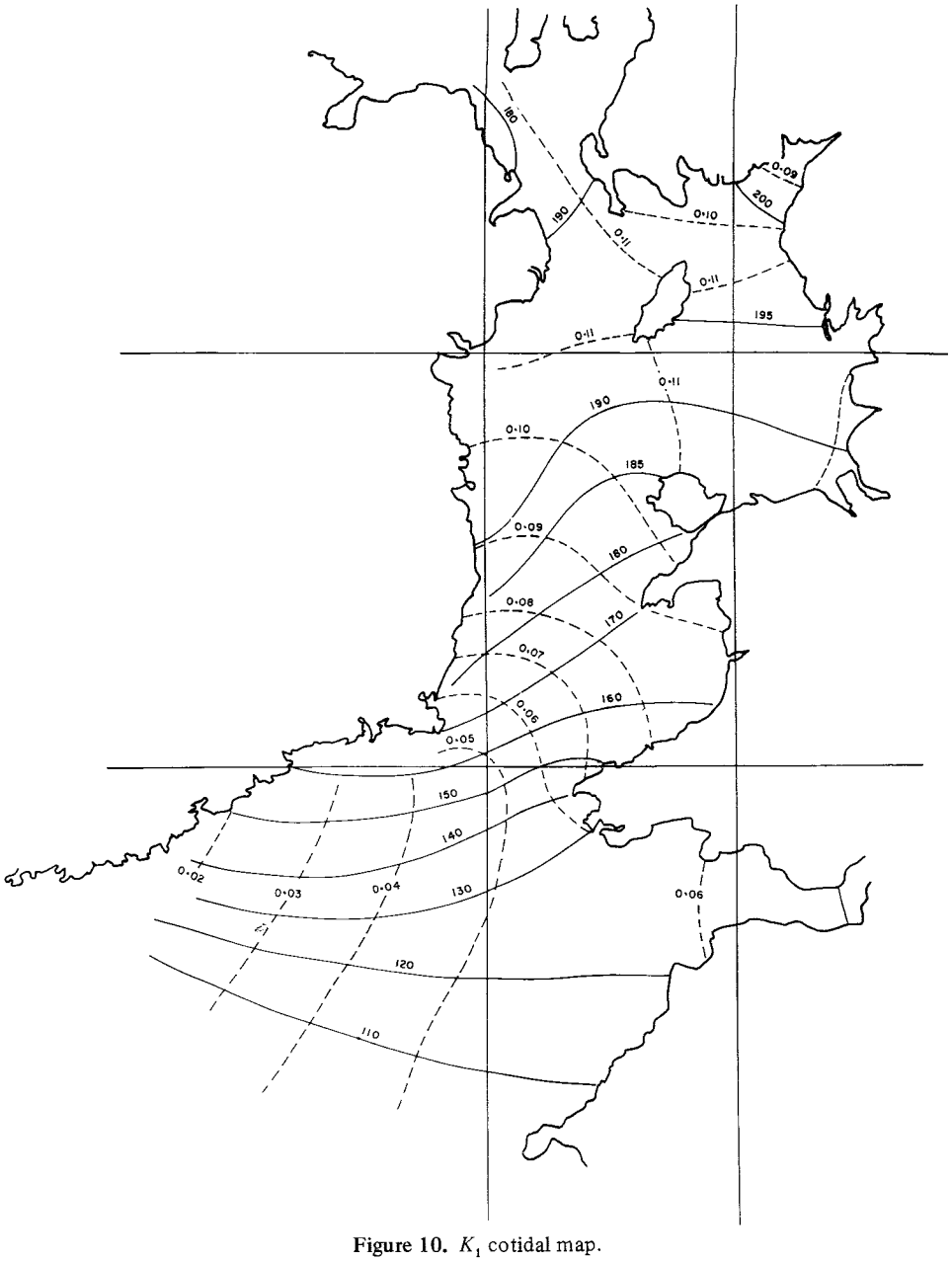

Figure 10. K_1 cotidal map.

therefore appropriate. The diurnal charts agree closely with the earlier German atlas, apart from a local increase in O_1 amplitude around the Isle of Man which could not be supported by the modern data. The amplitudes and the cotidal patterns of O_1 and K_1 are almost identical and describe an interesting tidal wave progression. As for the semidiurnal tides, the wave progresses from the south-west and through the North Channel to stand in the areas east of the Isle of Man. However, because the cotidal lines lie obliquely to the coast, the wave progresses from the Celtic Sea through St George's channel with its crest inclined

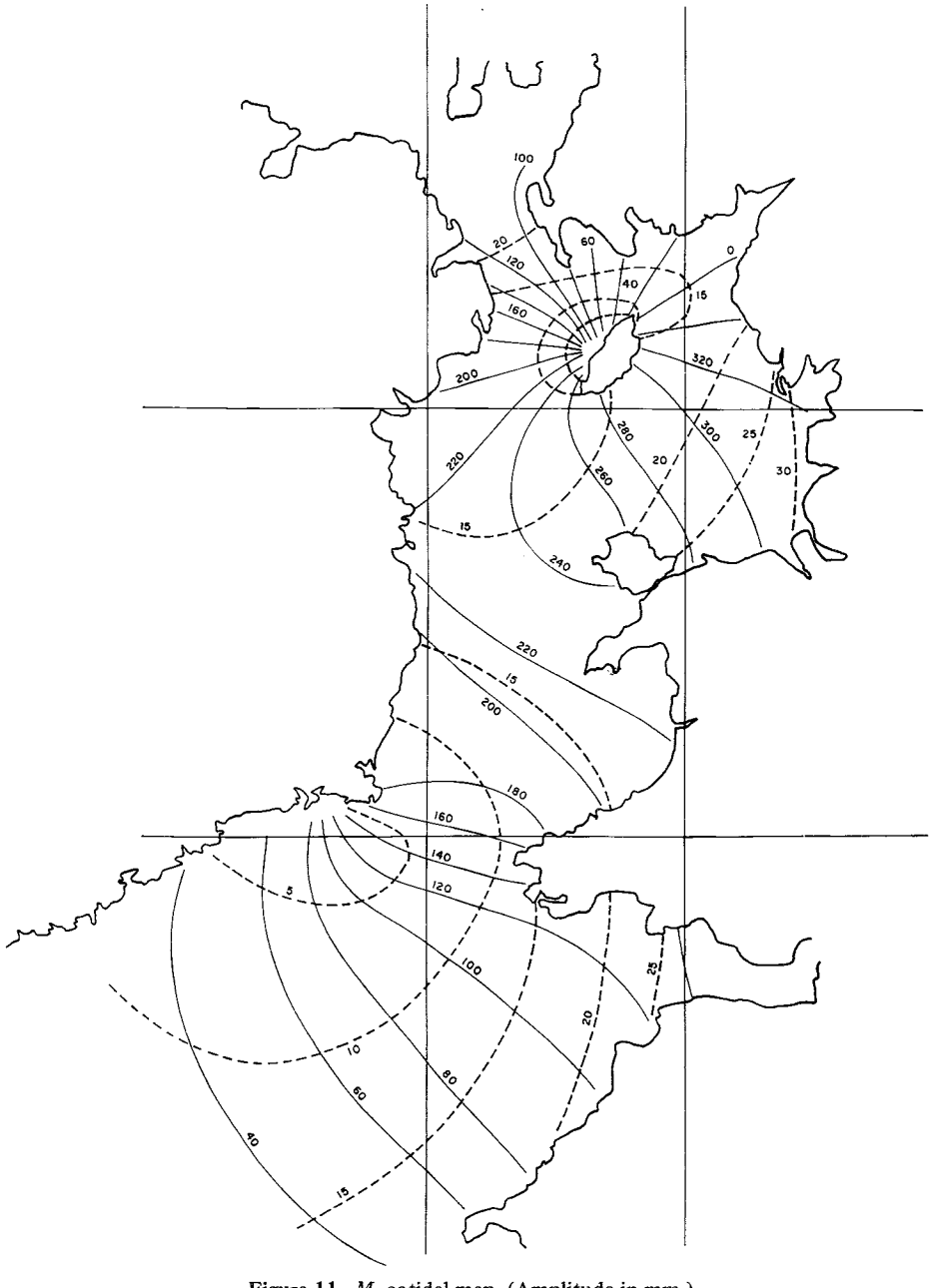

Figure 11. M_3 cotidal map. (Amplitude in mm.)

at approximately 45° to the direction of travel, steadily increasing in amplitude as it moves towards Liverpool Bay. Alternatively, because the cotidal and corange lines are nearly orthogonal, it may be envisaged as a type of Kelvin wave, the amplitude increasing to the right along the crests, which appears at the English coast, propagates in a north-westerly direction and disappears at the Irish coast.

The M_3 chart indicates a Kelvin-type wave progressing like the semi-diurnal tide from the Celtic Sea through St George's Channel, with the degenerate amphidrome in this case at

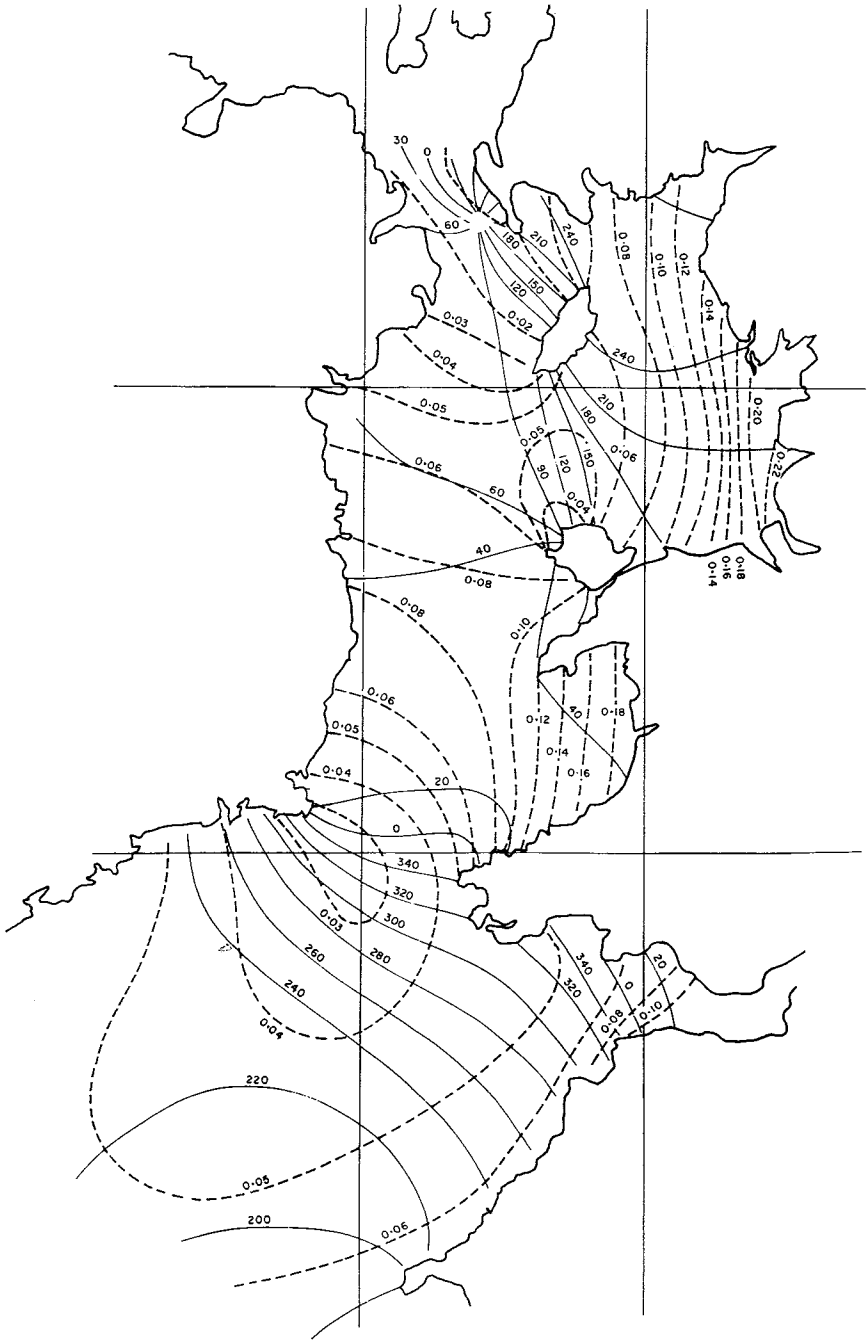

Figure 12. M_4 cotidal map. (Amplitude in m.)

Waterford rather than Wicklow, on the Atlantic side of Carnsore Point. When it reaches the northern Irish Sea, however, it appears to progress round the east of the Isle of Man, rather than standing like the lower frequency tides and, if the chart is correct, progresses right round the Isle of Man. M_4 also appears to progress in a Kelvin wavelike manner through the Celtic Sea. The rapid movement of the crest and the increase in amplitude between St

George's Channel and Anglesey suggest an input of energy in this vicinity, which is likely to be derived from the large semidiurnal currents associated with the degenerate elevation amphidrome. North of Anglesey, the pattern is complex and not confidently drawn, and it is likely that most of the energy in the system is generated locally. What is certainly clear from the data is that the smooth wave progression indicated in the early German charts bears little relationship with the real situation.

5 Tidal energy

A more complete understanding of the tidal dynamics of a shelf sea can be gained when information is available about the transmission and dissipation of tidal energy, as well as the kinematic information in the cotidal charts. In particular it is instructive to consider the mean over a periodic cycle of the energy flow associated with a particular tidal harmonic. If we neglect the effect of astronomical forcing and Earth tides, the time mean energy flux associated with a sinusoidal variation of elevation amplitude Z, phase ϕ_Z, and current amplitude V, phase ϕ_V is $\frac{1}{2}\rho g Z V \cos(\phi_Z - \phi_V)$, through unit area of vertical plane normal to the current direction. The energy flux in the east and north directions can therefore be readily calculated at each current meter site from the data prepared for the drawing of the cotidal charts. The vector sum gives the energy flux vector and this is plotted in Fig. 13 for M_2. Such a map clearly shows the overall flow of energy from the Celtic Sea northwards towards the east shore of the northern Irish Sea as expected from the progression of the tidal wave. It is interesting to note that a small amount of energy appears to flow west of the Isle of Man and out through the North Channel, although the single rig L_{69} may not be representative of the whole width of the North Channel. Another feature to note is the variation of mean energy directions between the top and bottom meters at certain places, particularly the Bristol Channel rig.

The total energy being transported at a particular station depends on the sea depth there, and so Fig. 13 does not give a true picture of the overall energy flow. The lines of current meter stations enable the total budget of energy flowing into a region to be calculated. Garrett (1975) has shown that the appropriate energy balance equation governing a region G is

$$-\int_M gh\overline{\mathbf{u}\zeta}\cdot\mathbf{n}\,ds + \int_M gh\overline{\mathbf{u}\zeta_E}\cdot\mathbf{n}\,ds + \int_G g\overline{\zeta_E\frac{\partial\zeta}{\partial t}}\,dA = \int_G \overline{\mathbf{F}\cdot\mathbf{u}}\,dA \qquad (5.1)$$

where $\mathbf{n}$ is an outward normal to an element ds of the open boundary M of the sea area G of which dA is an element.

ζ_E contains the effect of both astronomical tidal forcing and the motion of the solid Earth due to Earth tides and tidal loading. It is the height of an equipotential surface above its mean position, relative to the sea-bed. If U is the tide generating potential for the harmonic in question, then the Earth deforms such that the sea-bed rises a distance hU/g relative to the centre of the Earth (i.e. the Earth body tide), and the redistribution of the Earth's mass increases the tide generating potential by a factor k, where k and h are the tidal effective Love numbers normally taken as 0.29 and 0.59 respectively (Munk & MacDonald 1960). Thus the equipotential surface rises a distance $(1+k)U/g$ relative to the centre of the Earth, or $(1+k-h)U/g$ relative to the sea-bed. We may then write $\zeta_e = U/g$, as the equilibrium tide assuming a rigid earth with no Earth tides, and $\zeta_b = (k-h)U/g = -0.3\,U/g$ is the correction to this to allow for the body tide. There is a further contribution to ζ_E from the yielding of the Earth under the weight of the ocean tides; the load tide. This also consists of two parts corresponding to effective Love numbers k', h'. Farrell (1973) has

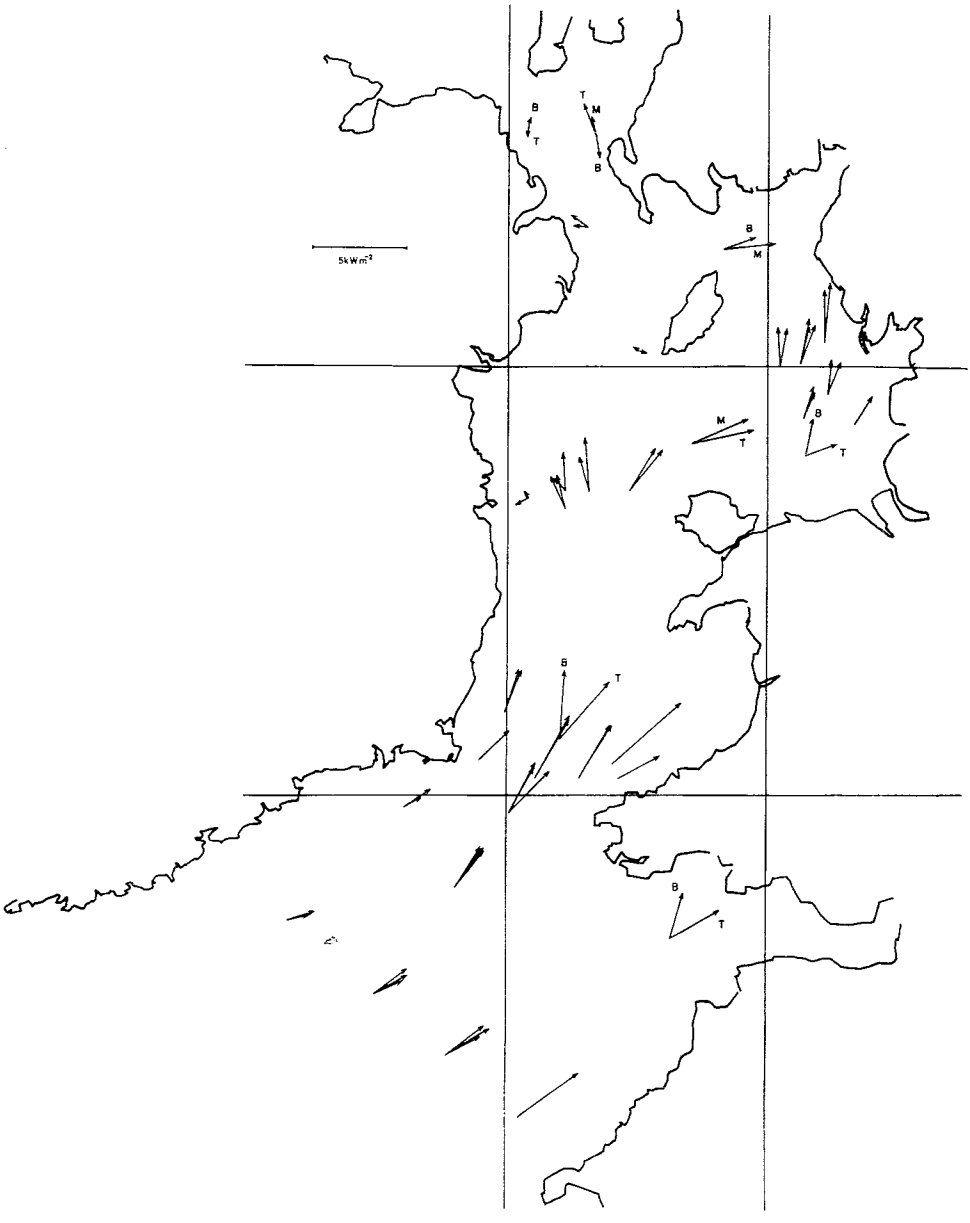

Figure 13. M_2 energy flux vectors, showing the mean over a tidal cycle. Where there is a significant difference, T = top meter, M = middle, B = bottom.

shown that the part due to perturbation in the Earth's gravity field because of the yielding is nowhere greater than 10 per cent of the part due to the vertical deformation of the surface. Moreover, in a shallow sea, the important spherical harmonics representing the loading will be of a high degree, which will result in $k' \ll h'$. k' can therefore be neglected, and if the height of the load tide is ζ_l relative to the centre of the Earth, $\zeta_l = h'U/g$. Thus neglecting the ocean self-attraction, we have $\zeta_E = \zeta_e + \zeta_b - \zeta_l$ representing the height of an equipotential surface relative to the sea-bed.

The first term of equation (5.1) corresponds to the apparent energy flux carried by the tidal wave into the area. It is the flux of potential energy measured relative to the sea-bed. The second term is best understood physically as a correction to the first, so that the combined term $-\int_M gh\mathbf{u}(\zeta - \zeta_E)\cdot\mathbf{n}\,ds$ represents the flux of potential energy measured relative to an equipotential surface. The third term is the work done on the sea in the area by virtue of the sea surface moving through a potential field which is itself varying with time. The term on the right side is the frictional dissipation term.

If we consider the mean energy associated with a particular tidal harmonic of frequency σ, and let

$$\mathbf{u}\cdot\mathbf{n} = U\cos(\sigma t - \phi_u)$$

$$\zeta = Z\cos(\sigma t - \phi_\zeta)$$

$$\zeta_E = Z_E\cos(\sigma t - \phi_E)$$

then

$$\overline{\zeta\mathbf{u}\cdot\mathbf{n}} = \tfrac{1}{2}UZ\cos(\sigma_\zeta - \phi_u) \tag{5.2}$$

$$\overline{\zeta_E\mathbf{u}\cdot\mathbf{n}} = \tfrac{1}{2}UZ_E\cos(\phi_E - \phi_u) \tag{5.3}$$

$$\overline{\zeta_E\frac{\partial\zeta}{\partial t}} = \tfrac{1}{2}\sigma ZZ_E\sin(\phi_\zeta - \phi_E). \tag{5.4}$$

If we parameterize bottom friction by a quadratic law, then $\mathbf{F} = \rho k\mathbf{u}|\mathbf{u}|$ and for rectilinear tidal streams of the form $\mathbf{u} = U_0\cos(\sigma t - \phi_v)$ where σ is the dominant tidal frequency,

$$\overline{\mathbf{F}\cdot\mathbf{u}} = \frac{4}{3\pi}k\rho U_0^3. \tag{5.5}$$

Substituting (5.2) to (5.5) in (5.1) enables the M_2 mean energy balance terms to be calculated throughout the Irish Sea from the current and elevation parameters already determined, provided ζ_E is known.

The area was divided by boundary lines as shown in Fig. 1 and the balance of energy evaluated in regions which are referred to as the eastern Celtic Sea, the southern Irish Sea and the northern Irish Sea. Across the St Ives–Cork boundary, the St George's Channel boundary and the Howth–Holyhead boundary there were several current meter rigs on or near the lines, in which case the line integral for apparent energy flux was obtained graphically from the plots of $UZ\cos(\phi_\zeta - \phi_u)$ and h across the section. These are shown in Fig. 14. Positive flux indicates energy flowing through the Irish Sea from south-west to north. The St Ives–Cork line reveals a typical Kelvin wave type of energy flux pattern, increasing in an exponential manner across the section, which can be integrated with some confidence to produce an energy estimate which should be accurate to within 5 per cent. Allowance was made for the lower energy flux indicated at the bottom meters, by assuming this flux to be appropriate to the bottom 10 per cent of the water column. There is less regularity of flux across the other boundaries, with some ambiguity off Fishguard arising from the flux associated with rigs E_{74} and L_{71}, both of which do not lie exactly on the St George's Channel section line chosen. There is no clear difference between bottom and top meters in this section. The Howth–Holyhead section is regular in the western half increasing eastwards from a negative (southward) flux off the Irish coast, but in the east it is not clear how to extrapolate the lines for 35 km where no meters were present. The given estimate is based on the line as drawn. Fortunately the sea is not at its deepest over this region and the

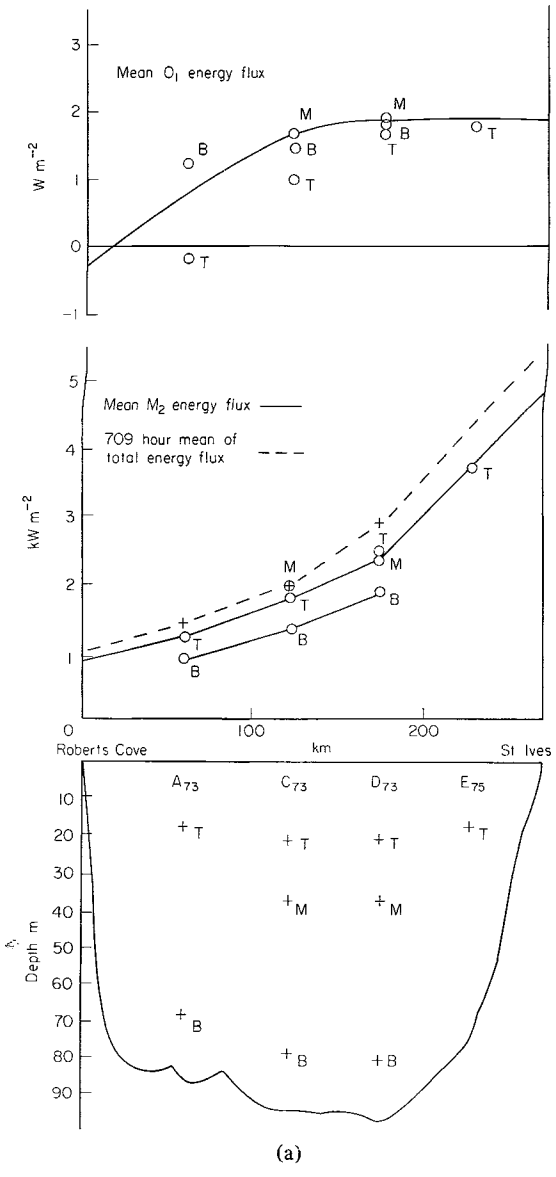

(a)

Figure 14. Energy sections. (a) St Ives to Cork line. (b) Carnsore Point to Fishguard line. (c) Howth to Anglesey line.

overall error is therefore unlikely to be more than 10 per cent, but further observations in this gap would be useful. For the North Channel and the Bristol Channel entrance, only one rig was on the section and it was necessary to assume it to be representative of the whole section. The estimates of apparent mean M_2 energy flux are shown in the first column of Table 6.

A similar method was used to estimate the magnitude of the second term in equation (5.1). The three contributions to this were evaluated separately. The equilibrium tide ζ_e is obtained directly from the astronomical variables, and has an amplitude of 10 cm decreasing to 8 cm from south to north of the area being considered and a phase between

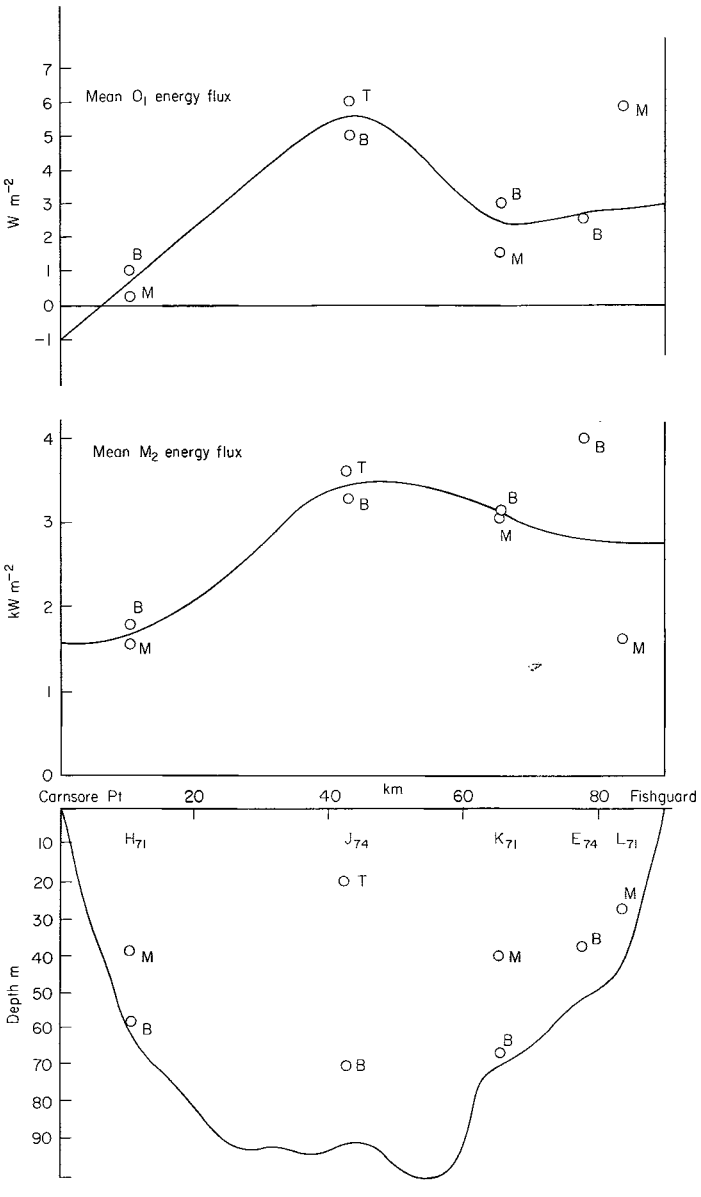

Figure 14 (b)

$-16°$ and $-8°$ relative to the Moon's transit at Greenwich. The body tide correction term, ζ_b, has an amplitude of 0.3 times the equilibrium tide and is 180° out of phase. The load tide ζ_l has been obtained from recent models of crustal loading by Baker (1977) and Bower (1970). Over the northern Irish Sea the load tide is very small and its contribution to the flux has therefore been ignored. It increases southwards to an amplitude of over 4 cm in the Celtic Sea, where it is almost 180° out of phase with the sea tide. Table 6 shows that, whilst these correction terms are much smaller than the apparent energy flux, they are certainly not insignificant, and it is important to include them in consideration of the energy budget.

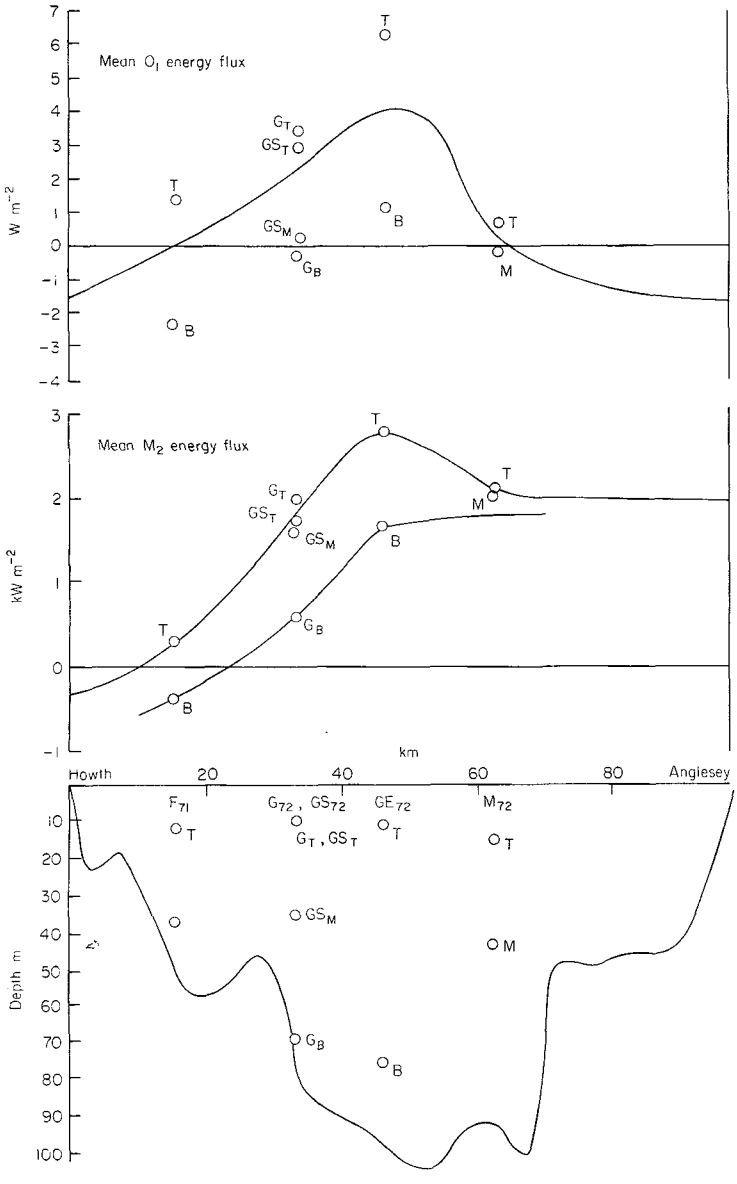

Figure 14 (c)

The third term of equation (5.1) was evaluated using (5.4), by measuring areas with a planimeter on a special 'cotidal' map representing ZZ_E as the amplitude and $(\phi_\zeta - \phi_E)$ as the phase. By taking sufficiently small intervals of amplitude and phase to define each area, an accuracy of about 5 per cent could be achieved. This was also evaluated in two stages, once for the equilibrium tide, from which the body tide follows, and once for the load tide. Because the amplitude of load tide in the northern Irish Sea is very small, and there is also rapid spatial variation of phase, it was assumed that the contribution to this area was negligibly small. The results of this spatial integration are shown in the first three rows of Table 7. When the fluxes across the lines are included to obtain the net energy flowing into an area, it is seen that the overall effect of the correction terms is a small reduction of the

Table 6. Mean M_2 energy flux across lines. Units are 10^6 kW (positive indicates flow northwards through the Irish Sea).

Line	Apparent energy flux in tidal wave	Correction from equilibrium tide	Correction from earth body tide	Correction from earth load tide	Net mean flux
St. Ives - Cork	44.9	0.26	-0.08	-1.13	44.0
Bristol Channel	7.2	-0.16	0.05	0.03	7.1
St. George's Channel	18.9	1.77	-0.53	-0.28	19.9
Holyhead - Howth	11.5	1.13	-0.34	negligible	12.3
North Channel	2.6	-0.23	0.07	negligible	2.4

apparent energy. As Garrett (1975) has pointed out, because the scale of ζ_e and hence the body tide are much greater than the size of the sea area, the flux terms and the surface integral terms tend to cancel out each other. This is not true for the load tide, however, although its overall effect is nonetheless very small.

The net inflow of energy must be absorbed by frictional dissipation in the area. An estimate of this was obtained using (5.5), by measuring areas on the map of U^3 shown in Fig. 4. k was taken as 0.002, the value used by Taylor (1919), and the results are presented in the bottom row of Table 7. Allowance was made in Liverpool Bay for the slight increase in frictional dissipation because the current ellipse is quite fat. It is immediately clear that the estimated friction is insufficient to account for the energy inflow into each area. For the southern Irish Sea, the discrepancy is only 4 per cent, within the limits of the accuracy of the calculations. In the northern Irish Sea it was noted at the current meter stations along the Fylde coast and off Morecambe Bay that the energy flux vectors have a significant component towards the shore, indicating a loss of tidal energy, as might be expected, within Morecambe Bay and in the estuaries along the Lancashire coast. Because the U^3 plots are based on the offshore currents, and make no attempt to allow for local topographic currents, no estimate can be made of the frictional losses along the coast in the above method. If, however, the energy flux towards the shore at stations A_{72}, B_{72} and D_{72} is integrated as a coastal frictional loss, a further 2.6×10^6 kW is accounted for, and the total loss is within 5 per cent of the net inflow of energy. This highlights the problem of performing this type

Table 7. Energy budget Irish Sea areas. Units are 10^6 kW (positive indicates work done on the sea by external forces).

	Celtic Sea	Southern Irish Sea	Northern Irish Sea
Work done by equilibrium tide on sea area	1.99	-0.81	-2.03
Work done by earth body tide on sea area	-0.60	0.24	0.61
Work done by earth load tide on sea area	0.26	0.14	negligible
Total work done on sea area	1.65	-0.43	-1.42
Net inflow of energy from equilibrium and earth tides	-0.18	-0.26	-0.47
Net inflow of tidal wave apparent energy	18.8	7.4	8.9
Net inflow of true energy	18.6	7.1	8.4
Estimated dissipation for k = 0.002	4.2	6.8	5.4
			(+2.6 in Morecambe Bay and Lancashire coast)

of energy budgeting as a means of estimating a correct value for k. It is never clear how much energy is lost in estuaries where the water is very shallow, although in the Irish Sea it is reasonable to suppose that coastal losses will be much larger along the Lancashire coast and in the Solway than where the coast is less indented with estuaries. In the southern Irish Sea, where the tidal currents are large away from the coastline, the effect of the coast can probably be neglected. It therefore seems that $k = 0.002$ is a reasonable friction coefficient to choose, but that 0.0021 might be a better value. Because energy dissipation is proportional to U^3, the energy budget is dominated by the high-velocity areas, and small errors in the contours of Fig. 4 could have a very large influence on the estimate of k.

Further inaccuracy arises in the budget from the places where only one rig was used to define a line. In the North Channel, where the energy flow is low, this does not affect the budget too badly, although it would be interesting to know if energy flows north or south through the Channel. However, in the Bristol Channel the problem is acute. The rig D_{75} in the Bristol Channel indicates a complicated vertical structure of energy flux and accurate definition of energy flux probably requires a line of rigs across the Channel. This could account for the very bad discrepancy for the Celtic Sea in the energy budget, which takes a value of 7.2×10^6 kW flowing into the Bristol Channel. Turning to literature for other estimates of M_2 energy loss in the Bristol Channel, Miller's (1966) estimate of 28×10^6 kW would be more than sufficient to balance the 14.4×10^6 kW of excess energy in the Celtic Sea balance. However, Bennett (1975) calculates a flux of 8.4×10^6 kW passing up the estuary at Minehead and a further 2.9×10^6 kW dissipated between Wormshead and Minehead, a total of 11.3×10^6 kW. Grace (1936) also studied tidal friction in the Bristol Channel and, although he did not calculate any fluxes, an estimate can be obtained from the figures for currents and elevations which he presented. These give a flux across the Wormshead section of only 4.5×10^6 kW, although an estimate of frictional dissipation between Wormshead and Weston-super-Mare, based on Grace's figures for bottom friction forces, yields 8.9×10^6 kW. A value around 10^7 kW seems reasonable, and this will not be sufficient to balance the budget. However, because the currents are low in the Celtic Sea, the bottom friction is low so that the neglect of what may be comparatively large losses at the coastline due to strong local currents off headlands and in estuaries may also be a significant source of error in the Celtic Sea energy budget.

The overall M_2 energy flow into the Celtic Sea, i.e. the flux across the St Ives–Cork line, is probably accurate to within 5 per cent, and can be compared with the other estimates in the literature. At 44×10^6 kW it is lower than Miller's value of 60×10^6 kW and more in agreement with the figure of 38×10^6 kW quoted by Miller for Heiskanen's estimate of frictional dissipation. The flux of 19.9×10^6 kW through St George's Channel agrees well with both Jeffreys' (1921) and Heiskanen's estimates of 20×10^6 kW for the Irish Sea proper. Taylor (1919) took his section line between Arklow and Bardsey Island, across the centre of the southern Irish Sea. His result of 64×10^6 kW was based on Spring-tide conditions. Assuming an $S_2 : M_2$ ratio of 0.35 for both currents and elevations, this would correspond to an M_2 flux of 35×10^6 kW or twice what is observed using these data. This shows the difference that can be made to the calculation of energy flux by using more reliable and detailed data, and gives an indication of the typical errors which may be present in estimates of global tidal energy dissipation such as Miller's, which of necessity must be derived from crude tidal observations.

Apparent flux calculations were also made for S_2 and O_1, and these are presented in Table 8. The flux cross sections for S_2 were similar to M_2 and are not shown, but the O_1 profiles can be seen in Fig. 14 to differ considerably from M_2, with a southward flux at the west coast and northwards flux over the rest of the section.

Table 8. Apparent energy flux in O_1 and S_2 tidal waves.

Line	O_1 10^3kW	S_2 10^6kW
St. Ives - Cork	30.1	7.02
St. George's Channel	23.1	2.16
Bristol Channel	not clear from one station	1.01
Holyhead - Howth	8.1	1.58
North Channel	4.5	0.27

Table 9. Apparent energy flux across line between stations A_{73} and D_{73}.

Energy in M_2 tidal wave	19.59×10^6 kW
Energy in S_2 tidal wave	3.16×10^6 kW
Energy in O_1 tidal wave	1.7×10^4 kW
709 hour mean of hourly instantaneous energy flux	23.62×10^6 kW

Because the currents at A_{73}, C_{73} and D_{73} were obtained simultaneously with elevations at Roberts Cove, St Ives and C_{73}, the instantaneous apparent energy fluxes could be calculated at the three rigs, including both the potential energy term and the kinetic energy term which disappears in the mean for a single harmonic. As time series, these showed a strong quarter cycle periodicity as expected. Their mean was taken over 709 hours, i.e. two Spring–Neap cycles, the result representing approximately the mean tidal apparent energy flux into the Celtic Sea contained in the major constituents. From the values at the three rigs a profile across the section was constructed (see Fig. 14(a)) but because simultaneous elevation and current data were not available at E_{75}, the eastern part of the profile is guesswork. To compare the total flux into the area with the fluxes of M_2, S_2 and O_1, therefore, only the flux across the centre portion of the line between A_{73} and D_{73} was considered – see Table 9. M_2 and S_2 account for over 96 per cent of the total energy flux and it is likely that the semidiurnal band of tidal harmonics contains over 99 per cent of the tidal energy flow into the Celtic and Irish Seas. Some caution must be exercised in this comparison, however, because the individual harmonic estimates are based on constants which are independent of the nodal tidal variations whereas the instantaneous flux calculations include the nodal tide effects. This is equivalent to observing that the total energy flux can be represented as the sum of energy fluxes in individual harmonics, as demonstrated by Pugh & Vassie (1976), only if we are considering the total energy flux averaged over a period of time equal to or very much greater than the longest period tidal fluctuation of any significance, i.e. the 18.6-yr nodal period.

6 Conclusions

The overall conclusion which can be drawn from this study is that the collection of current meter data over periods of 14 to 28 day or more enables the tidal dynamics of a region to be charted in detail, not only for the principal tidal harmonic but also for all the major constituents in the diurnal and semidiurnal species, provided a sufficient network of coastal tide gauges is available. In respect of the cotidal maps presented here, it is suggested that minor improvements should be possible if current meters were placed north-west of the Isle of Man, between Wicklow and the Lleyn peninsular, and in the east of the Celtic Sea

between Milford Haven and St Ives. Coastal gauges between Wicklow and Rosslare would also clarify the location of the semidiurnal degenerate amphidrome.

The plotting of cotidal maps for shallow water tides is much less precise. Such maps have little value in describing the dynamics of tides generated within the region, but should they be required for navigational or engineering purposes, the use of offshore tide gauges is essential in the exercise described here since it bypasses the problem of the coastal records, dominated by local effects, being unrepresentative of the offshore conditions.

The siting of current meters in a line between coastal tide gauge stations, especially when an offshore tide gauge is also situated on the line, has been shown to provide very useful and reliable information about tidal energy flux, particularly where synoptic records were obtained as across the St Ives–Cork line. It appears that the plotting of energy sections is essential for accurate estimation of the energy flux, and further observations across the Bristol Channel and the North Channel lines would be very valuable. Corrections for the tide generating forces, and the effect of Earth tides are also seen to be worth making since the accuracy of energy estimates obtainable from a well-placed line of current meters and tide gauges should be ± 5 per cent. The drawing up of an energy budget from which an estimate of the bottom friction coefficient can be made is seen to be less reliable in view of the uncertainty about the contours of high velocity and the amount of energy dissipated at the coastline. Given these reservations, and making an informed estimate of the coastal dissipation, a quadratic bottom friction coefficient of 0.0021 achieved an energy balance within 5 per cent for the Irish Sea. However, the uncertainties encountered in calculating the frictional dissipation in this way, despite the good coverage of velocity data, implies that reliable estimates of global tidal energy dissipation will only be made when sufficient tidal current and elevation data are available around the continental margins for direct calculations to be made of energy flux into the shallow seas.

Acknowledgments

The author is indebted to his former colleagues at I.O.S., Bidston, who were involved in obtaining and processing the data used in this study. He also wishes to acknowledge the help of Mr John Ramster in supplying current meter data collected by the Fisheries Laboratory, Lowestoft.

References

Alcock, G. A. & Vassie, J. M., 1975. *Offshore tide gauge data,* Institute of Oceanographic Sciences, Data Report No. 7.

Baker, T. F., 1977. *Earth Tides Crustal Structure and Ocean Tides,* Eighth International Symposium on Earth Tides, Bonn, in press.

Baker, T. F. & Lennon, G. W., 1977. The interaction of marine tides and crustal structure with the earth tide signal in N.W. Europe, *Ann. Geophys.*, **33,** p. 173.

Baxter, G. C. & Bedwell, J. A., 1972. The MAFF current-meter system and data inventory, 1968–71, *MAFF Fish. Lab. Techn. Rep. Ser. No. 4.*

Bennett, A. F., 1975. Tides in the Bristol Channel, *Geophys. J. R. astr. Soc.*, **40,** 37–43.

Bowden, K. F., 1955. Physical oceanography of the Irish Sea, *MAFF Fish. Inv. Ser. II,* Vol. **XVIII,** No. 8.

Bower, D. R., 1970. Some numerical results in the determination of the indirect effect, *Communs. Obs. r. Belg. A9 (Ser. Geophys. 96),* p. 106.

Defant, A., 1961. *Physical Oceanography,* vol. II, Pergamon, Oxford.

Doodson, A. T. & Corkan, R. H., 1932. The principal constituent of the tides in the English and Irish Channels, *Phil. Trans. R. Soc. A,* **231,** 29–53.

Doodson, A. T., Rossiter, J. R. & Corkan, R. H., 1954. Tidal charts based on coastal data, *Proc. R. Soc. Edin. A*, **64**, 90–111.

Farrell, W. E., 1973. Earth tides, ocean tides and tidal loadings, *Phil. Trans. R. Soc. Lond. A*, **274**, 253–259.

Flather, R. A. & Heaps, N. S., 1975. Tidal computations for Morecambe Bay, *Geophys. J. R. astr. Soc.*, **42**, 489–517.

Garrett, C., 1975. Tides in gulfs, *Deep-Sea Res.*, **22**, 23–35.

Godin, G., 1972. *The Analysis of Tides*, University of Toronto Press.

Grace, S. F., 1936. Friction in the tidal currents of the Bristol Channel, *Mon. Not. R. astr. Soc. Geophys. Suppl.*, **3**, 388–395.

Heaps, N. S. & Jones, J. E., 1975. Storm surge computations for the Irish Sea using a three-dimensional numerical model, *Mem. Soc. r. Sci. Liège, ser. 6*, **7**, 289–333.

Howarth, M. J., 1975. Current surges in the St. George's Channel, *Est. Coast. Mar. Sci.*, **3**, 57–70.

Howarth, M. J. & Loch, S. G., 1973. Institute of Coastal Oceanography and Tides, *Data Rep. No. 3.*

Howarth, M. J. & Loch, S. G., 1974a. Institute of Oceanographic Sciences, *Data Rep. No. 3.*

Howarth, M. J. & Loch, S. G., 1974b. Institute of Oceanographic Sciences, *Data Rep. No. 4.*

Howarth, M. J. & Loch, S. G., 1974c. Institute of Oceanographic Sciences, *Data Rep. No. 6.*

International Hydrographic Bureau, 1974. *Tides–harmonic constants–index of stations*, Special Publication No. 26, (loose leaf sheets, updated to 1974).

Jeffreys, H., 1921. Tidal friction in shallow seas, *Phil. Trans. R. Soc. A*, **221**, 231–264.

le Provost, C., 1973a. Decomposition spectrale du terme quadratique de frottement dans les equations des marées littorales. Method d'analyse, *C. r. Acad. Sci. Paris Ser. A*, **276**, 571–574.

le Provost, C., 1973b. Decomposition spectrale du terme quadratique de frottement dans les equations des marées littorals. Résultants, *C. r. Acad. Sci. Paris, Ser. A*, **276**, 653–656.

Marineobservatorium Wilhelmshaven, Hamburg, 1942. Karten der harmonischen Gezeitenkonstanten für das Gebiet der Westbritischen Gewasser, *Ausgabe A*, 1805A.

Miller, G. R., 1966. The flux of tidal energy out of the deep oceans, *J. geophys. Res.*, **71**, 2485–2489.

Munk, W. & MacDonald, G. J. F., 1960. *The Rotation of the Earth*, Cambridge University Press.

Proudman, J. & Doodson, A. T., 1924. The principal constituent of the tides of the North Sea, *Phil. Trans. R. Soc. A*, **224**, 185–219.

Pugh, D. T., 1971. *Sea level measurements using the Neyrpic Bubbler Pressure Gauge*, Institute of Coastal Oceanography and Tides, Internal Report No. 22.

Pugh, D. T. & Vassie, J. M., 1976. Tide and surge propagation off-shore in the Dowsing Region of the North Sea, *Duet. Hydr. Zeit.*, **29**, 163–213.

Ramster, J. W. & Howarth, M. J., 1975. A detailed comparison of the data recorded by Aanderaa and Plessey recording current meters, *Deut. Hyd. Zeit.*, **28**, 1–25.

Sager, G. & Sammler, G., 1975. *Atlas der Gezeiterstrome für die Nordsee, den Kanal und die Irische See*, 3rd edn, Seehydrographischer Dienst der Deutschen Demokratischen Republik, Rostock.

Simpson, J. H., Hughes D. G. & Morris, N. C. G., 1977. The relation of seasonal stratification to tidal mixing on the continental shelf, in *A Voyage of Discovery*, pp. 327–340, ed. Angel, M., Deep-Sea Res. Supp.

Taylor, G. I., 1919. Tidal Friction in the Irish Sea, *Phil. Trans R. Soc. A*, **220**, 1–33.